Enhancement of a Rolling Resistance Rig for Force and Moment Testing of Tires

Surabhi Suhas Ramdasi

Thesis submitted to the faculty of the Virginia Polytechnic Institute and State University

in partial fulfillment of the requirements for the degree of

Master of Science

In

Mechanical Engineering

Saied Taheri (Chair)

Corina Sandu

Robert West

May 3rd 2016

Blacksburg, VA

Keywords: tire testing machine, force and moment test, rolling resistance test, cleat test, tire positioning mechanism, loading mechanism

Enhancement of a Rolling Resistance Rig for Force and Moment Testing of Tires

Surabhi Suhas Ramdasi

ABSTRACT

Tire testing has been one of the important aspects of the tire industry because it helps identify the tire behavior which further helps in improving the design of tires. It also helps automotive manufacturers choose the best tire for their automobiles. Indoor tire testing helps in relating the data better because of greater repeatability of the testing setup as compared to outdoor testing. This study focusses on modifying a rolling resistance machine to make it capable of force and moment and cleat testing along with the standard rolling resistance test. Additionally, the design of a mechanical loading mechanism (used to apply normal force on the tire) in place of the previous one using dead weights is also discussed.

This study also talks about the structural and vibrational finite element analysis of a tire testing machine. Since the machine was designed to conduct different tire tests, different structural requirements of the tire positioning mechanism pertaining to each test were taken into consideration, and the structure was analyzed for maximum forces and moments acting on the assembly. Cleat testing subjects the tire as well as the structure to an impulse force which calls for the vibrational analysis of the assembly to avoid the structure from resonating.

The design was modified to get it easily manufactured and assembled. These design changes and the aspects taken into consideration have also been discussed.

GENERAL AUDIENCE ABSTRACT

A tire is an indispensable part of any bicycle, moped, car, truck or pretty much every vehicle we see on the road on a daily basis. Pneumatic tires are the most common tires and consist of a rubber casing filled with air. These tires act as a supporting structure for the vehicle chassis as well as provide some isolation to the driver from the shocks arising from the terrain the vehicle is travelling on. Thus, the tires play an important role in deciding the ride quality of the vehicle. Many different types of tires exist in the market and they tend to behave differently under different circumstances. Generally, a vehicle is designed based on the forces and moments the tire will transmit to the vehicle while travelling on the road. Hence, tires need to be tested in an environment which closely reflects the conditions they are supposed to work in. In an indoor tire testing facility, the road surface is simulated using different materials. Other parameters affecting the tire performance like tire pressure, tire temperature, speed, load can be controlled within a permissible range to reflect the actual on-road conditions. Also, it is much easier to test the tires for extreme conditions in an indoor testing facility. Additionally, because the tire parameters are closely monitored, the testing can be done much faster than conducting actual on-road tests. Thus, indoor tire testing machines play an important part in studying the tire characteristics in a much safer environment and at a lower cost. The data obtained from these tests can be effectively used for design of vehicles and for tire research purpose. An indoor tire testing facility was designed and developed to test passenger car tires and light truck tires and also to aid the future research projects at Center for Tire Research.

ACKNOWLEDGEMENTS

I would like to thank my academic adviser, Dr. Saied Taheri, for giving me a chance to work on this research project at CenTire (Center for Tire Research) and for his valuable guidance throughout the past two years. I would also like to thank Dr. Ronald Kennedy and Dr. Robert West for their timely inputs to improve the various technical aspects of this project. Additionally, I would like to thank my colleagues, Tariq Abuhamdia, Eric Pierce and Sheetanshu Tyagi for helping me with the various aspects of the design.

I would like to thank Dr. Corina Sandu for her participation in my thesis committee.

Finally, I would like to acknowledge the technical support offered by Dr. Gerald Potts and everybody else from Test Measurement System Inc. (TMSI). Their valuable feedback helped steer the project in the right direction. I would also like to thank 'Maxon Precision Motors' and 'Michigan Scientific Corporation' for their financial support.

Table of Contents

List of Figures

List of Tables

CHAPTER 1: Introduction

The pneumatic tire came into existence in mid 1800s. After the advantages of pneumatic tires were recognized, they found a place in nearly every automobile running on the roads. Being a critical component of any automobile manufactured, the tire impacts the properties of the automobile to a great extent. The forces and moments acting on the tire under different conditions play an important role in the automobile design industry. The tire industry needs to manufacture more durable and efficient tires with the growth of the automobile industry. This makes tire testing an important part of the tire as well as automotive industry. Different testing setups are available for measuring the forces and moments generated by the tire, rolling resistance of tires, endurance testing of tires, uniformity testing of tires along with a few procedures which allow for outdoor testing. Tire testing machines have been around since early 1900s, but, with the advent of new technologies and better measurement systems, new machines are being designed every day to cater for the market needs.

This work talks about a new tire testing machine designed to conduct force and moment test, rolling resistance test and cleat test for passenger car tires and light truck tires. The design of the machine and the concept behind it has been developed based on the machines that have been manufactured and are running successfully and also depending on the standard guidelines for different tests.

This document is organized as follows:

Chapter 1 talks about the background of tire testing and focusses on the details pertaining to indoor tire testing also discussing a few other perspectives of the research.

Chapter 2 emphasizes on the generation of the design concept. It presents the restrictions, scope and criteria for this particular machine.

Chapter 3 outlines the actual design of the machine and discusses the function of each individual component and the perspective behind the design.

Chapter 4 addresses the analysis of the design. The chapter elaborates on vibrational and static structural analysis of the design using finite element analysis approach.

Chapter 5 investigates the design from the Design for Manufacture (DFM) perspective. It highlights the changes made to the design to make it suitable to get manufactured. Finally, chapter 6 summarizes the work done in this thesis and elaborates briefly on the work which can be done in the future.

1.1 Need of Tire Testing

As mentioned earlier, pneumatic tires are a mandatory part of nearly every automobile manufactured in today's era. Thus, a tire plays an important role in the comfort and safety of the passenger driving an automobile. Tires show different characteristics based on their tread pattern, ply, material, inflation pressure etc. Tire testing is the cheapest and fastest way to evaluate the performance of a tire. Different tire properties are studied using the data generated from tire testing. A few examples of tire testing machines are: tire force and moment machine, rolling resistance machine, uniformity machine, tread wear simulation machine and tire endurance testing machine.

Forces and moments arising from a tire help decide the ride and handling of a vehicle. Hence, the data generated using these tests is used in designing the suspension systems. This data is also helpful in developing mathematical tire models.

Rolling resistance of a tire adversely affects the fuel efficiency of a vehicle. With fuel efficiency being one of the most critical aspects regarding the popularity of a car, automotive manufacturers want it to be as low as possible. The energy lost in overcoming the rolling resistance can be determined by doing rolling resistance tests and also the impact of different parameters like tire inflation pressure, tire temperature and the normal load acting on the tire can be studied for a tire.

Uniformity testing helps identify the roundness of a tire. It also helps determine the forces generated because of runout or an imbalance in the tire. Endurance testing of tires helps identify the durability of tires and these tests typically run for long durations which might go up to weeks of testing time. A few other tests are carried out on tires depending on the need of the tire manufacturer and based on the demand of the automotive manufacturer.

1.2 Comparison of Indoor and Outdoor Tire Testing

Tire testing can be done indoors – on a test machine, or it can also be done outdoors – on actual roads or testing tracks. Even though outdoor testing is more realistic and can provide a better representation of the condition the tire is supposed to operate in, it also has some disadvantages.

Previous studies claim that outdoor testing encounters the following problems [1]:

i. The car and the wind noise is a hindrance while conducting tire noise tests.
ii. There is no control over environmental factors, like temperature, which can affect the interpretation and repeatability of data.
iii. Generally, tire testing needs to be done in extreme conditions, like high slip and camber angles, large normal loads and very high speeds. Achieving these conditions in an indoor testing setup is much easier and safer than doing it outdoors.
iv. For indoor test setups, maintaining the coefficient of friction is easier as compared to outdoor facilities because the test surface to be maintained is limited.

In 1978, comparative rolling resistance tests were carried out for the same tires on indoor and outdoor facilities [2]. Analysis of variance for all the facilities in which the rolling resistance tests were conducted has been shown in the figure below:

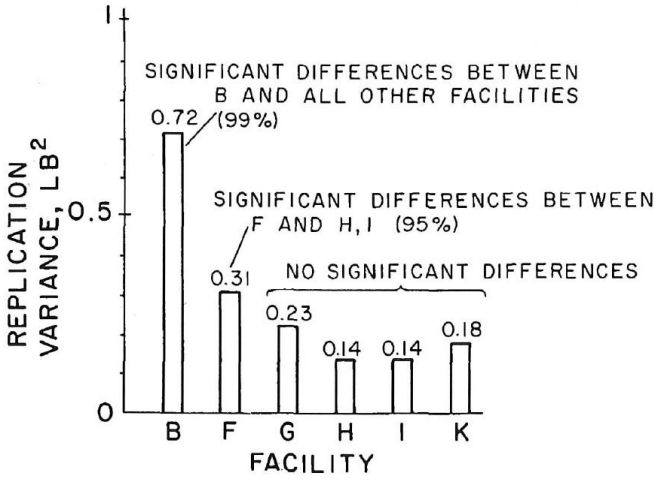

Figure 1: Comparison between Indoor and Outdoor Facilities [2].
Used under fair use 2016.

In the above figure, facility B is an outdoor testing facility and facilities F, G, H, I and K are indoor testing facilities. Facility B was seen to show much less precision than the rest of the facilities, the reason being more variables affecting the tire performance than indoor facilities. The indoor facilities showed an average standard deviation of 0.44 lb. and the outdoor facility showed a standard deviation of 0.85 lb. The reason for the reduced precision in case of outdoor testing facilities is explained by the following parameters [3]:

i. Test surface texture: Indoor tire testing is generally conducted on sand paper which has a uniform friction coefficient as opposed to the road surface. Also, contaminants present on the road surface affect data measurements because the tire loses contact with the road.
ii. Temperature: The ambient temperature is very important in determining the tire parameters. Indoor testing helps in controlling these environmental factors but for outdoor testing the temperature depends on the weather which leads to inconsistency in tire parameters. It might also affect the data acquisition system used in the wheel transducer.
iii. Vehicle Drift: There is a possibility of the vehicle drifting in the outdoor tests because of wind or because of differences in driving of the vehicle. This uncertainty is negated for indoor testing of tires.

In conclusion, indoor tire testing facilities show much better precision and repeatability as compared to outdoor testing because of much better control of environmental factors.

1.3 Effect of Measuring Surface

Tire testing is either done on a flat surface or a drum. The curvature of the drum affects the contact patch and thus, is not a correct representation of the surface profile the tire normally runs on. Previous studies present conflicting results about the effect of the drum curvature on the measured tire forces and moments. Even though the rolling resistance obtained using drums is less than the values obtained using a flat surface, conversion factors have been developed to successfully convert the drum values to flat surface values.

One of the earliest comparisons for drums and flat surfaces was conducted by testing the tires on a 67.23" drum covered with alundum cloth [4]. These results were compared with the ones obtained by placing a wooden plank between the tire and the drum such that the plank was rigidly fixed in place. The plank was covered with alundum cloth as well. The plots from this study have been shown below:

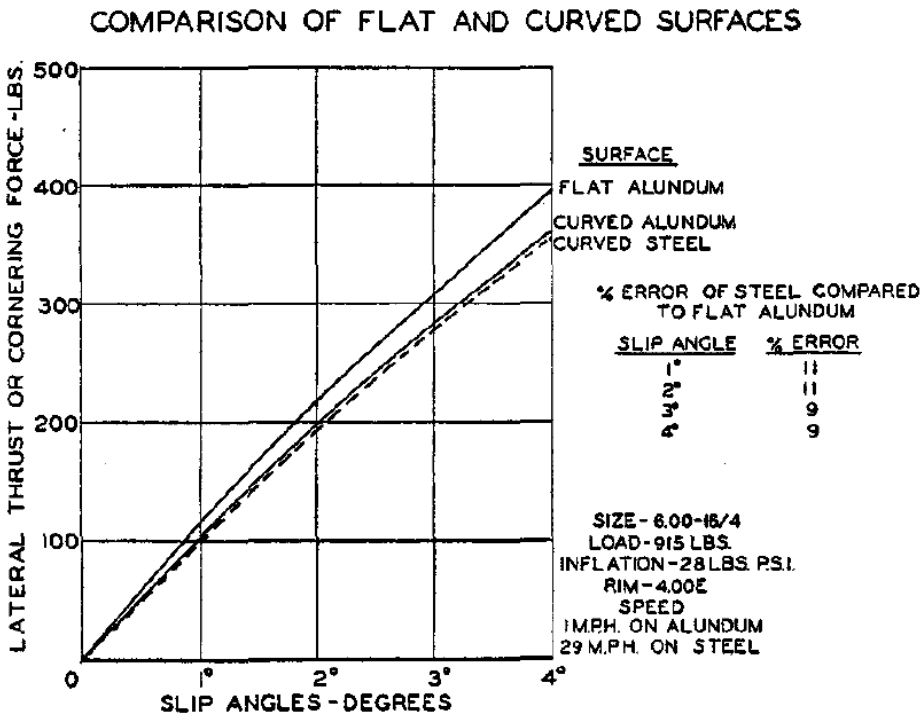

Figure 2: Effect of Surface Curvature on Cornering Force [4].
Used under fair use 2016.

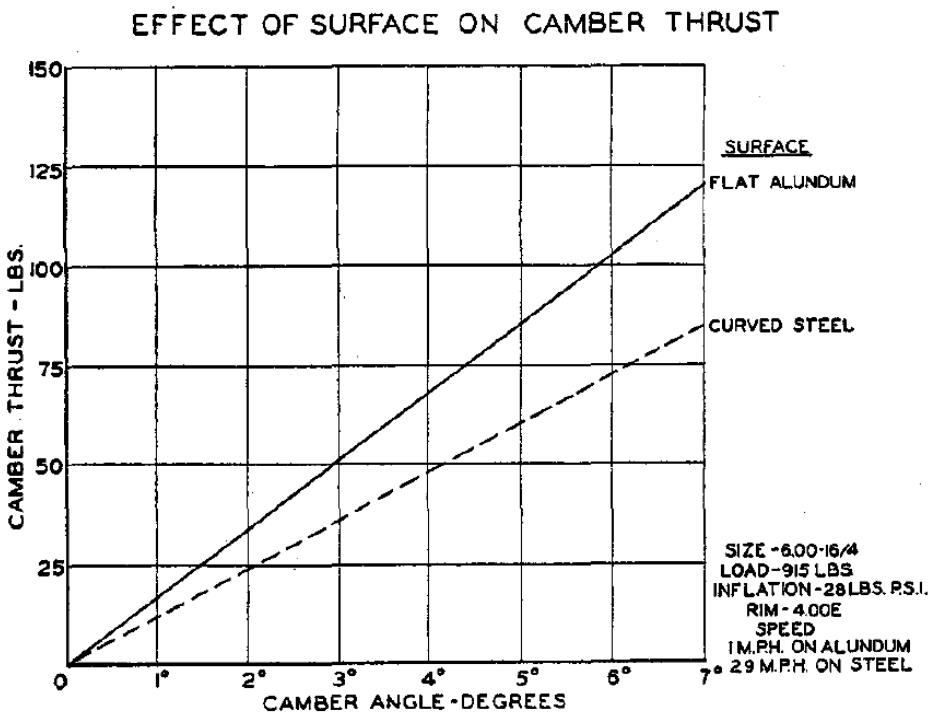

Figure 3: Effect of Surface Curvature on Camber Angle [4].
Used under fair use 2016.

The results from the study showed that the self-aligning moment was nearly the same for a curved surface as well as a flat surface. A small, insignificant difference in values for lateral force was observed – the force measured on a curved surface being lower than that on a flat surface. A significant difference in the values of camber thrust was obtained for both the surfaces, but, the overall value of camber thrust being small as compared to the cornering force, this difference, according to the author does not impact the measurements to a large extent.

A few other studies found a difference of zero to 25-30% in the values obtained on a drum and a flat surface, but no definite correlation exists between data obtained using a curved surface and a flat surface.

Another comprehensive study done in 1976, compared the data obtained using a drum with a machine using a flat belt for the same tires. Significant difference in lateral force for both the surfaces was observed at low slip angles, but the difference reduced with increase in slip angle. This study also showed a similar trend of lower camber thrust in case of curved surface. In conclusion, the effect of the surface curvature of a

drum is to give reduced values of cornering force and camber thrust, but a definite relationship between the values is a function of the individual tire and no generic conversion factor has been found to convert the values into data representative of a flat surface.

On the other hand, the rolling resistance is shown to increase with decreasing drum diameter as shown in the figure below[1] [2]:

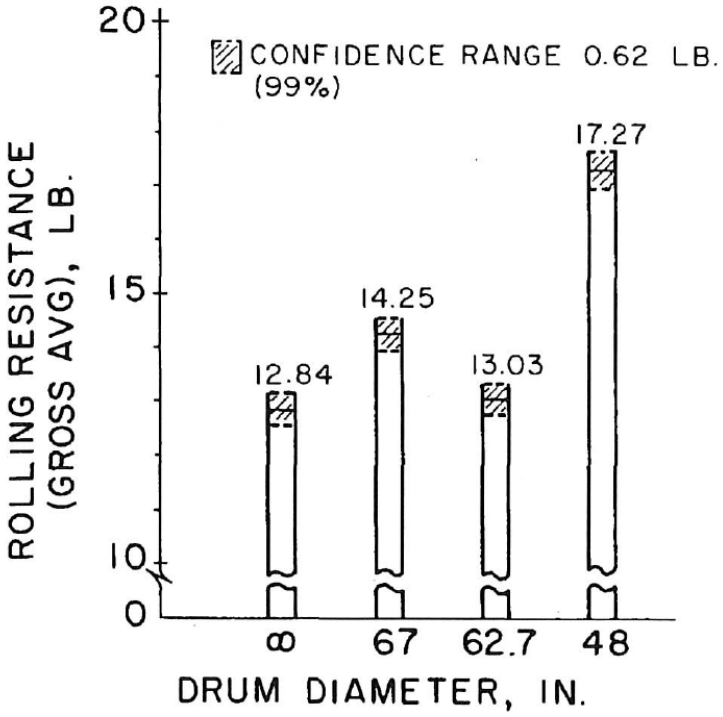

Figure 4: Average Rolling Resistance for a Tire on Different Surfaces [2].
Used under fair use 2016.

As the rolling resistance is considered a function of tire deflection, rolling resistance values are higher on smaller drums owing to higher deflection of the tire contact patch. Based on the assumption that rolling resistance is proportional to deflection, S. K. Clark derived the following relation to convert the data obtained on a curved surface to a flat surface:

$$F_{rd} = F_{rf}\left(\sqrt[2]{\left(1 + {}^{d}/_{D}\right)}\right) \quad (1)$$

[1] With the exception of 62.7" drum data. Authors of the article are unsure about the reason for the discrepancy in the data.

Where, F_{rd} is the rolling resistance on a drum, F_{rf} is the rolling resistance obtained using a flat surface, d is the tire diameter and D is the diameter of the drum used in testing machine.

Equation (1) is shown to give good precision for passenger car tires. Based on this assumption, Luchini developed a similar relation for truck tires[5].

Also, the SAE standards [6] for steady state force and moment testing of tires suggest that the only considerable difference between the contact patch for a flat and curved surface is the contact patch length. Contact patch width only slightly differs for the two interfaces.

1.4 Review of Tire Testing Machines

Indoor tire testing is being done since the 1930s. A few researchers (Evans, Bull) tried to find the tire forces and moments using a drum. In 1958, Gough was responsible for doing one of the first force and moment tests on a flat surface using a wooden plank. This was done more regularly in 1960s and better flat testing surfaces were introduced in the form of a tensioned belt driven over two rollers. Today, quite a few facilities have belt driven flat surface machines and a few also use drums.

A brief summary of the most important advances in the field of tire testing machines is as follows:

In 1939, Bull tested tires on a machine which used drums [4]. The tire could be positioned at different slip and camber angles on the drum. The loading mechanism utilized a dead weight system. Along with force and moment testing, this machine was capable of conducting cleat tests. The results from this study were helpful in obtaining the fundamental relationships between the tire forces and moments and the different input variables.

In 1962, Gough and Whitehall published an article about a tire testing machine which mounted the tires using two platforms [7]. One of the platforms was oriented with respect to the other platform using six screw jacks. Out of the six screw jacks, every two were mounted in a plane so as to rotate and translate the tire in all six degrees of freedom. The machine used a flat moving platform for the testing.

In the same year, the B. F. Goodrich tire dynamics machine was designed [1]. It consisted of two different stations – one for testing of passenger car tires and one for light and heavy truck tires. The tire positioning mechanism was capable of aligning the tire at different slip and camber angles on a drum driven by a motor. This machine also had the provision of measuring the rapid steering response of the tire, which was done by driving the tire with the help of a D.C. motor capable of providing sinusoidal variation.

In 1963, Nordeen and Cortese designed a machine which used a movable flat table on which the tire could be positioned at different camber and slip angles under different normal loads using servo controlled hydraulic actuators [8]. This machine was also capable of separately providing a driving or a braking torque to the tire using a motor.

In 1967, Ginn and Marlowe came up with a modified design of the B.F. Goodrich machine and made it capable of accommodating passenger, light duty and heavy duty truck tires [9]. Also, instead of a drum, this machine used a surface driven by a rack and pinion for testing the tires on a flat surface. In 1970, Dugoff and Brown modified the flat bed B.F. Goodrich machine design with a stronger loading frame and a supporting foundation to make it more suitable for testing truck tires [10].

Ritter and Kristofetz came up with a design in 1972 capable of measuring the tire forces and moments on a flat belt [11]. The tire was loaded using hydraulic actuators. The camber angle for the tires had to be changed manually though. The machine had the provision to control the tire steer using hydraulic actuators.

In 1973, the Calspan Tire Research facility was developed by Bird and Martin [12]. This is one of the most popular and widely used tire testing facility. The design used an endless steel belt supported over two drums. The belt was supported on air bearings to provide the required stiffness to the belt against deformation from the tire contact patch. The drums supporting the belt and the tire-wheel assembly were driven using a hydraulic motor. The tires could be tested on different frictional surfaces using different steel belts. The tire positioning system used hydraulic motors to align the tire at the required position on the belt. The tire positioning mechanism also had the capability of positioning the tire onto one of the drums used for supporting the belt to conduct tests on drum surface as well.

In 1980, Langer and Potts developed a flat surface tire testing machine commonly known as the Flat-Trac^{TM} machine [13]. This machine is capable of conducting force and moment test, rolling resistance test and dynamometer tire test. This design utilized an A-frame capable of pivoting about a point on the test surface for the slip and camber angle change. The radial positioning of tires was also done with respect to the A-frame. The testing surface used a belt driven over two drums. This is one of the most commonly used commercial machines for tire testing.

Similar to the Flat-Trac^{TM} machine, another design was developed to conduct rolling resistance on a flat surface by Lloyd in 1978 [14]. This machine was solely developed to measure the rolling resistance and had no provision of slip and camber angle change of the tire. The machine was capable of testing passenger and light duty truck tires on a flat surface supported on hydrodynamic bearings. In addition to the rolling resistance test, this design also had the provision to conduct uniformity test and revolution per kilometer tests for tires.

In the past few decades, many advances have been done in the field of tire testing machines. With better instrumentation options and advanced control strategies, data acquisition has improved considerably. Also, many testing setups are capable of conducting different tire tests on flat surface machines. Many testing facilities use the external and internal surface of drums to conduct multiple tests at one time.

1.5 Research Motive

A rolling resistance machine was donated by TMSI (Test Measurement System Inc.) to CenTire (Center for Tire Research) at Virginia Tech. This machine was redesigned and remodeled to conduct the force and moment test, rolling resistance test and cleat test on passenger car and light duty truck tires.

The motive behind remodeling the machine was to be able to use it for university research. There are very few tire testing facilities in North America and most of them are a part of major tire companies and automotive industries. It is very expensive to get the tires tested at these facilities. In addition, the entire data related to a particular tire model is very rarely available for external research purposes.

This machine would provide CenTire with an in-house source to obtain tire data. Additionally, it would be much faster to obtain different data sets pertaining to different conditions and parameters which will help in developing empirical tire models. In future, the machine is also going to be used for conducting noise tests on tires, and for studying the tire footprint. Vibrational analysis and endurance testing of tires using cleats can also be done on the same setup.

1.6 Research Objectives

- To design a tire testing machine capable of conducting force and moment test, rolling resistance test and cleat test of tires which includes a tire positioning mechanism and a loading mechanism
- To be able to test passenger car tires and light truck tires on the setup
- To accommodate the entire design on the previous rolling resistance machine base, which was donated by TMSI and also to ascertain that the new setup is manufactured and built at a lower cost as compared to the machines available in the market
- To implement industry specified standards and guidelines for tire testing into the design
- To validate the design for strength and vibrations using finite element analysis methods
- To implement the controls and relevant interfaces for the machine for accurate data acquisition and testing repeatability
- To manufacture and assemble the machine and improvise the design from the manufacturing perspective (DFM)
- To verify the ability of the machine to conduct the tests with the required precision and accuracy

1.7 Review of Tire Tests

a. Force and moment testing of tires has been prevalent since the past century. The forces and moments obtained from the test setup help in designing the ride and handling of the vehicles on which the tire is being used on. The variations in tire

forces and moments also affect the directional control of the vehicle. Additionally, the data acquired from these tests is used in developing mathematical tire models. These models are mostly semi-empirical models and in fact need a few parameters which are determined using the actual data obtained from force and moment testing of tires. This test is preferably carried out on flat surfaces. The setup for this test needs to be capable of measuring the three orthogonal forces and three orthogonal moments acting on the tire. The input variables for this test are – slip angle, camber angle and normal load acting on the tire. During testing, generally, one of the input variables is changed and the rest are kept constant. A few other properties affecting the force and moment testing are: effective rolling radius, tire spin velocity and road velocity, loaded radius, temperature, surface profile and coefficient of friction.

The apparatus for this testing setup consists of three different parts: a measuring surface to simulate the road; generally a flat belt driven on two rollers, a tire positioning mechanism to adjust the slip and camber angle of the tire and a loading mechanism to apply the normal force on the tire.

b. Rolling resistance test helps in determining the energy lost by the tire while running on a surface. Rolling resistance affects the fuel efficiency and can impact the emission targets for a vehicle. Rolling resistance test is carried out by loading a tire against a frictional surface at a zero slip and zero camber angle.

Rolling resistance can be measured using the following methods:

i. Force method: in this method, the rolling resistance is obtained by measuring the force acting on the tire spindle. The disadvantage of this method is a high possibility of cross-talk between the measured forces which might lead to some errors in measurement. The SAE standard for rolling resistance tests [15] gives the rolling resistance as follows:

$$F_R = F_x\left(1 + {}^{R_L}/_{R}\right) \tag{2}$$

Where, F_R is the rolling resistance, F_x is the measured spindle force, R_L is the loaded radius of tire and R is the test wheel radius.

ii. Torque Method: in this method, the rolling resistance is obtained by measuring the torque required by the test measurement system to keep the tire speed constant. Some error might be obtained in the data measured because of the torque fluctuations of the system.

$$F_R = {}^{T}/_{R} \tag{3}$$

Where, T is the input torque of the system.

iii. Power Method: rolling resistance is obtained by measuring the input power required by the test setup. This test needs to be carried out with minimum fluctuation in surface speed to minimize the error in the obtained values of force.

$$F_R = {}^{P}/_{v} \tag{4}$$

Where, P is input power for the measurement system and v is the speed of the test surface.

The force value obtained from keeping the tire in skimming contact with the drum surface is subtracted from the above values of F_R to get the actual value of rolling resistance.

c. Cleat testing helps in determining the tire response and its ability to absorb energy when excited by an impulse. This test is generally carried out on a drum (1.7 m or more) and the tire is excited with the help of a metal bar attached to the drum surface either perpendicular or oblique to the direction of tire rotation. The cleats are mounted on the drum surface one at a time. The wheel transducer used in the testing setup needs to be capable of measuring three forces (longitudinal force, lateral force and normal force) and two moments (overturning moment and aligning moment) which are developed when the tire rolls over the cleat. The loading mechanism in the test setup needs to be rigid enough to sustain the high forces arising from cleat test to avoid any backlash.

CHAPTER 2: Design Concept Generation

A rolling resistance machine donated by Test Measurement System International (TMSI), Inc. was redesigned and remodeled to make it suitable for force and moment testing of passenger car and light truck tires. The machine has a 1.7 m (67.2 inches) diameter drum driven with the help of a 60 HP D.C. motor and capable of going up to 80 mph. The face width of the drum is nearly 300 mm (12 inches).

The new testing setup was designed based on the requirements for the different tire tests. Also, since the objective was to use the same mounting base and the drum (testing surface) available on the original rolling resistance machine, the space constraints were defined.

2.1 Specifications of the Original Machine

The original machine had the capability to conduct only rolling resistance tests. It consisted of a drum and an arm to load the tire against the drum. The loading mechanism for the machine used dead weight and a lever system to apply normal load on the tire.

The new design was modified to obtain added testing capabilities on the same setup and to implement better instrumentation systems as compared to the nearly obsolete ones on the original machine.

A comparison of the specifications for the old and the new machine has been enlisted in the table below:

Table 1: Comparison of Specifications

Parameter	Old Machine	New Machine
Drum Speed	80 mph	80 mph
Tire Rim Sizes	-	14” – 17”
Camber Angle Change	-	± 10°
Slip Angle Change	-	± 15°
Loading Mechanism	Dead weights and	Motor driven screw

	mechanical lever	
Tests Carried Out	Rolling resistance test	Slip test, cleat test and rolling resistance test

2.2 Design Criteria

The maximum values for the forces and moments for which the structural members of the frame have been designed were obtained based on the data presented in the previously published literature.

The maximum value of the normal force was ascertained based on the guidelines for cleat test. The guidelines specify the loading capacity to be twice that of the tire rating. Based on this criteria, the normal force was set at 25000 N.

The maximum lateral force acting on the assembly was estimated using the following plots:

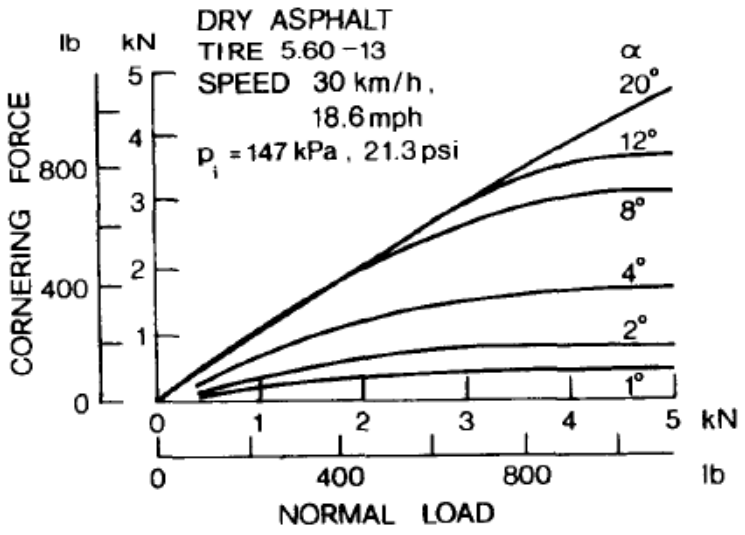

Figure 5: Cornering Force vs. Normal Load at Different Slip Angles for a Passenger Car Tire [16]. Used under fair use 2016.

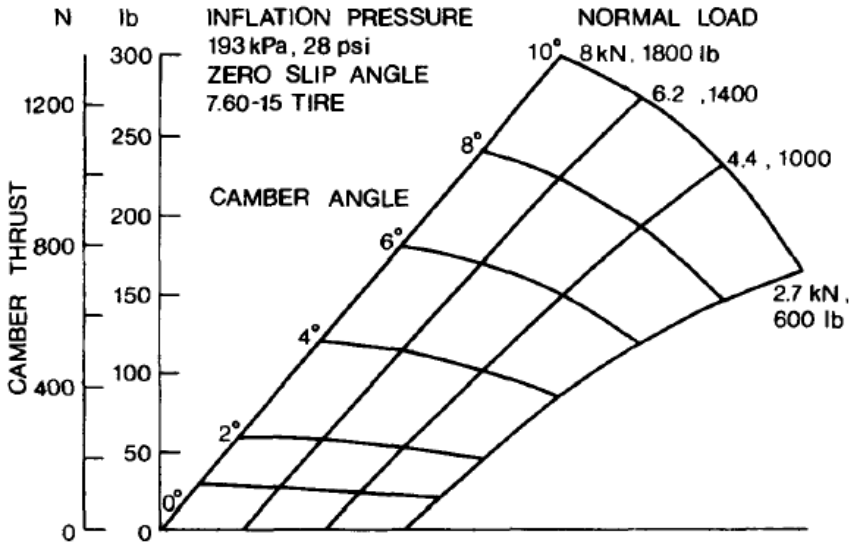

Figure 6: Camber Thrust at Different Values of Normal Load and Camber Angle [16].
Used under fair use 2016.

From the above plots, the maximum value of lateral force was estimated to be 5000 N.

The following plots were also taken into consideration:

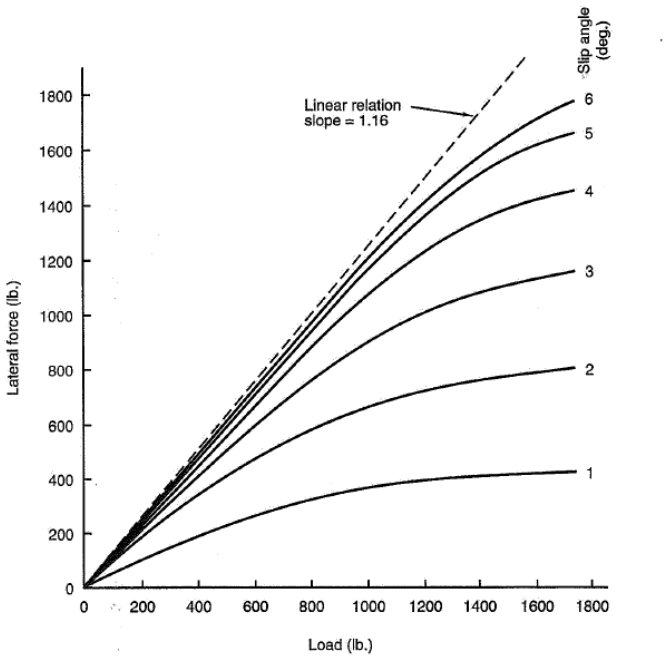

Figure 7: Lateral Force vs. Load at Different Slip Angles for a Race Car Tire [17].

Used under fair use 2016.

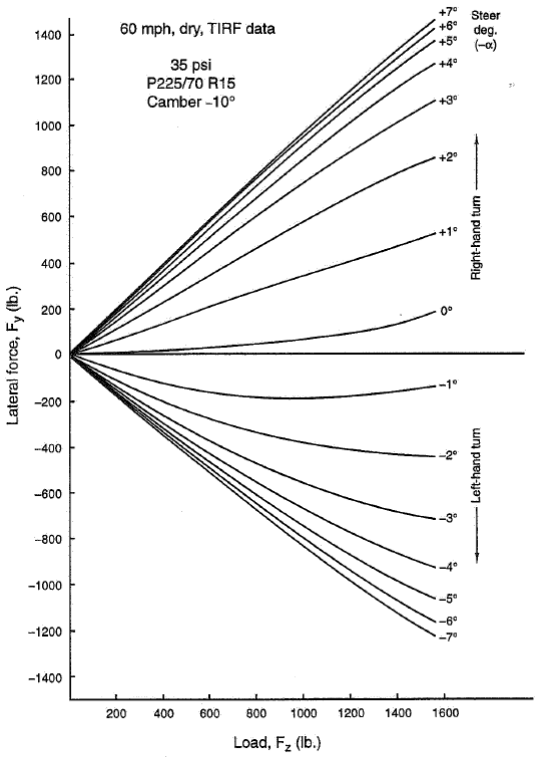

Figure 8: Lateral Force at Different Normal Loads and Slip Angles and Constant Camber Angle [17].
Used under fair use 2016.

The maximum values for lateral force from both the plots shown above is roughly 1400 lb. (6228 N). Thus considering all of the data shown above, and taking some factor of safety into account, the value of maximum lateral force was set at 12500 N. The aligning torque on the tire was estimated based on the following plots:

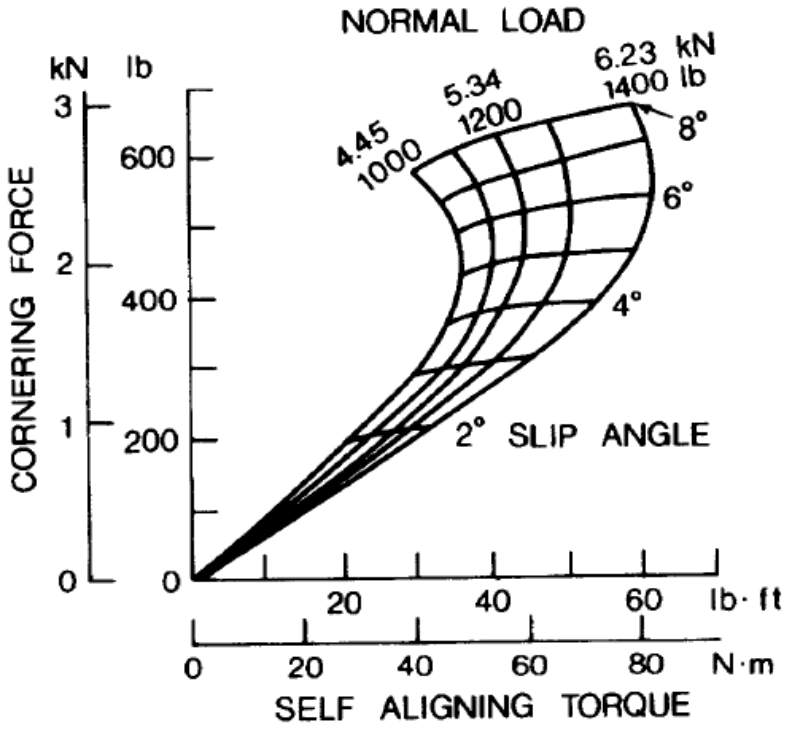

Figure 9: Variation of Cornering Force and Self Aligning Torque at Different Normal Loads and Slip Angles for a Car Tire [16].
Used under fair use 2016.

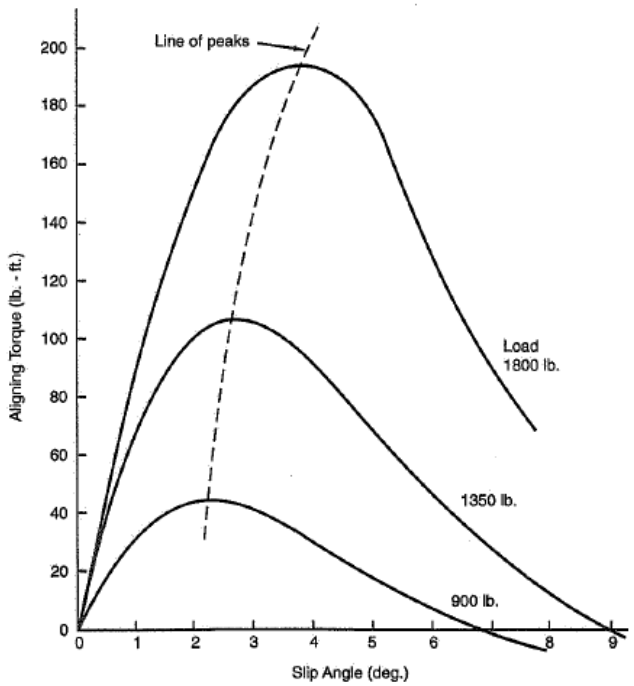

Figure 10: Aligning Torque vs. Slip Angle at Different Normal Loads for a Passenger Car Tire [17].
Used under fair use 2016.

Based on the plots, the maximum value of aligning moment is around 200 lb-ft (271 Nm). Thus, the design was done considering a maximum value of aligning torque to be 300 Nm.

The overturning moment was decided based on the following plots:

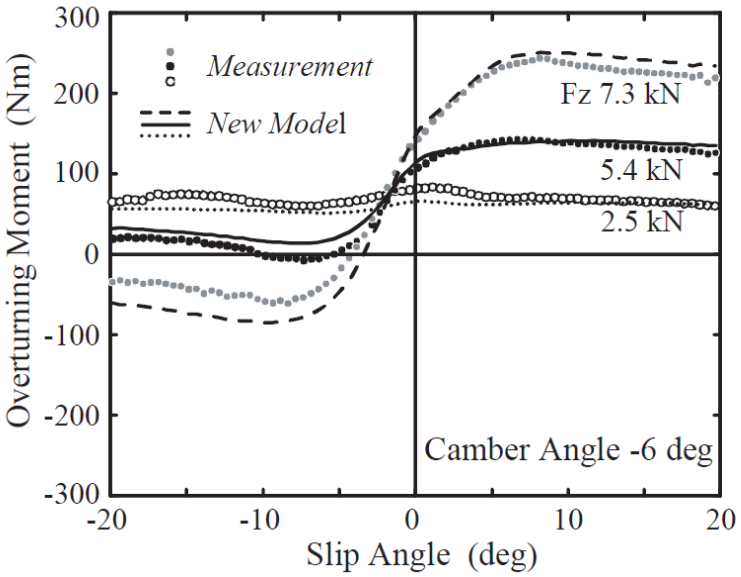

Figure 11: Overturning Moment vs. Slip Angle for a Passenger Car Tire [18].
Used under fair use 2016.

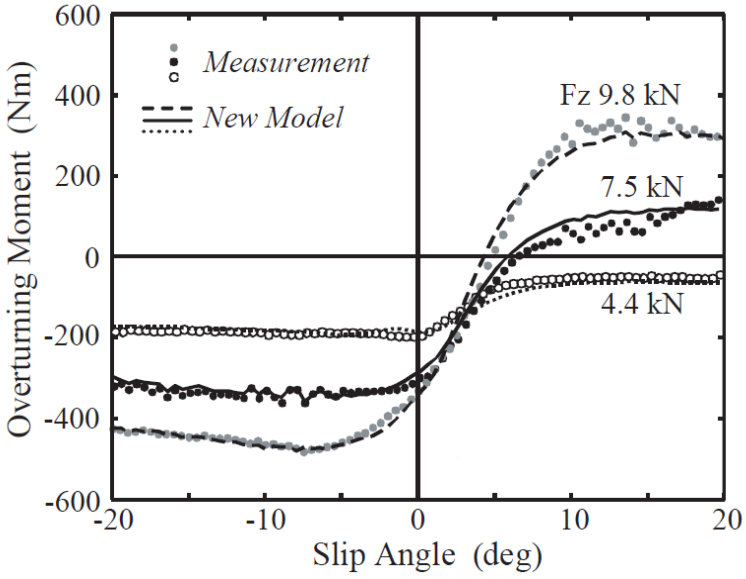

Figure 12: Overturning Moment vs. Slip Angle for a Light Truck Tire at a Camber Angle of 9° [18].
Used under fair use 2016.

Based on the plots shown, the maximum value for the overturning moment was estimated as 400 Nm.

The longitudinal force was assumed to be 15000 N and the rolling resistance moment was estimated to be 300 Nm (also referenced from plots found in previous literature). The maximum values of tire forces and moments for which the machine has been designed have been listed below:

Table 2: Force and Moment Measurement Capability

Tire Load	25000 N
Lateral Force	12500 N
Longitudinal Force	15000 N
Overturning Moment	400 Nm
Aligning Torque	300 Nm
Rolling Resistance Moment	300 Nm

2.3 Design Guidelines

Most of the design for the machine was done based on the guidelines given in the SAE standards for the individual tests.

Road simulation: the force and moment testing of tires is preferably done on a flat surface. In the past, before the flat surface machines were designed, considerable testing has been done on drums as well. The flat surface machines can be of two types: fixed road surface and moving tire or moving road surface and fixed tire. The length of road surface for a moving tire needs to be considerably long so that sufficient data is obtained at steady state of tire, thus, latter is the preferred option for force and moment testing. Rolling resistance tests are commonly carried out on drums (1.708 m is the most commonly used) and the data obtained is converted to flat

surface using Clark's relation. Cleat test is generally done on a drums, with sizes ranging from 1.7 m and up.

Testing Surface: the force and moment test and the rolling resistance test is ideally carried out on a medium coarse texture (80 grit sandpaper). Force and moment tests can also be carried out on a bare drum unless the tread surface becomes sticky. But, comparisons in the past have shown a lot of variation in the data obtained on textured surface and that for a bare drum. Cleat tests need to be carried out on a bare drum and cleats need to be secured on the drum surface using adequate fastening measures.

Speed: for force and moment testing, the steady state values for tires have been seen to be independent of speed unless the tire is sliding on the surface. Tests have been successfully carried out at speeds as low as 1 mph. For a rolling resistance test, the ideal speed to conduct the test is 80 mph. There is no guideline to conduct the cleat test at a particular speed, but the SAE standards for cleat testing mention speeds of 32.2 km/hr. and 64.4 km/hr. in the text [19].

Temperature: effects of temperature on force and moment tests have not been investigated. The rolling resistance test needs to be carried out in an ambient temperature of 20° C to 28° C. The obtained data needs to be converted to 24° C using the following relation [15]:

$$F_{RR} = F_R[1 + k(T_A - T_R)] \tag{5}$$

Where, F_{RR} is the corrected value of rolling resistance at the required temperature (N), F_R is the actual value of measured rolling resistance (N), T_A is the temperature during the test (°C), T_R is the temperature at which rolling resistance is to be calculated (°C), k is the temperature adjustment factor ($(°C)^{-1}$). The guidelines for cleat test specify the temperature range for cleat testing as 22° C ± 2° C.

Tire positioning system and loading mechanism: the tire positioning mechanism needs to align the tire at the required slip and camber angle for force and moment testing. On the other hand, this frame needs to be rigid enough to maintain the slip and camber angles within the required range of accuracy for rolling resistance and cleat test.

The required accuracies for slip and camber angle and the required range of the loading mechanism have been summarized in the table below:

Table 3: Comparison of Parameters Relevant to Force and Moment Test, Rolling Resistance Test and Cleat Test

Input Parameter	Force and Moment Test [20]	Rolling Resistance Test [15]	Cleat Test [19]
Slip Angle	Within ± 0.05° of the required angle	0 ± 0.1°	0 ± 0.05°
Camber Angle	Within ± 0.05° of the required angle	0 ± 0.3°	0 ± 0.05°
Normal Load	40-160% of tire rated load	Up to 100% of tire rated load	Twice the 100% load specified for the tire

CHAPTER 3: Design Development

The design of the machine was done in two parts – design of the tire positioning mechanism and design of the loading mechanism. The design of the tire positioning mechanism involved the provision to hold the tire against the drum and changing the slip and camber angle of the tire. The function of the loading mechanism is to apply a normal force on the tire. An alternative loading mechanism was designed to eliminate the cumbersome procedure of loading the tire using dead weights which were being used in the older mechanical loading mechanism. The other aspects of the design involved the various control strategies and data acquisition systems associated with the individual functions of the test setup.

3.1 Design of Tire positioning mechanism

The tire positioning mechanism is the part of the machine on which the tire and a force hub is going to be mounted to place the tire in contact with the rotating drum. This part of the machine is also used to control the input parameters – slip angle and camber angle. The mechanism needs to be able to change the slip and camber angles in ± directions up to required thresholds for force and moment testing. Additionally, the structure should have the sufficient structural rigidity to hold the slip angle within ±0.1° and the camber angle within ±0.3° for the rolling resistance measurement according to SAE J1269.

According to Langer and Potts (1980), it is beneficial if the radial positioning of the tire, the camber angle change and the slip angle change are uncoupled [13]. The tire positioning mechanism was designed based on this criterion so as to obtain better control of the input variables.

The tire positioning mechanism consists of the following components – force hub mount, ball screw supported between bearings on both sides inside the front box member, lateral beam, spline gearbox, rear box, supporting plates, reaction rod collar, reaction rod and truss members. The CAD model for the tire positioning mechanism has been shown in fig. 13.

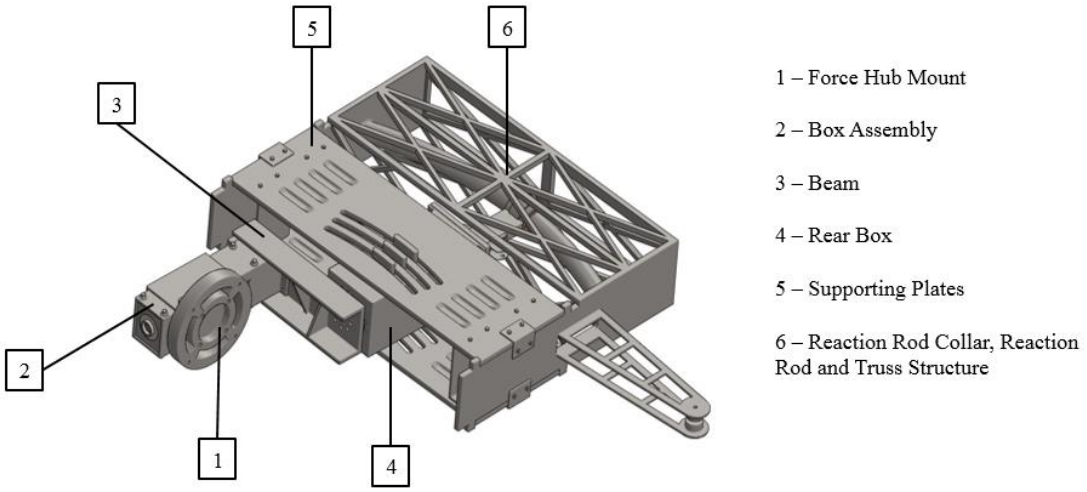

Figure 13: Tire positioning mechanism

The functions of the above mentioned individual components are as follows:

3.1.1 Force Hub Mount: The force hub mount is the part of the assembly on which the force hub and tire are mounted. The force hub is from 'Michigan Scientific Corporation' and is capable of measuring the forces and moments in all three directions. The assembly has a provision of mounting tire rim sizes ranging from 14" to 17" i.e. passenger car tires and light truck tires. The force hub mount is supported on the box member as seen in the figure shown below. The force hub mount is designed such that flanges on the backside of the mount go around the box member and thus help counter the twisting moment acting from the tire on it. These flanges help in reducing the effect of aligning torque which in turn helps in better control of the slip angle. The central cuboidal portion of the force hub mount is mounted over a nut.

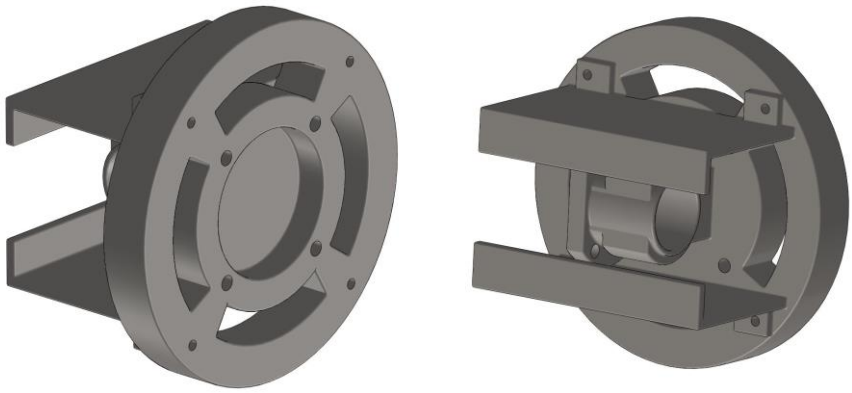

Figure 14: Force Hub Mount – Front and Back View

3.1.2 Force Hub and Wheel Assembly: Some modifications and extra components have been added to the force hub design to make it suitable for mounting different tires for conducting tests on the machine. A wheel hub (used in trucks and having a capacity of 12000 N at static condition) is connected to the front face of the force hub mount. An adapter was designed to make it possible to connect the rotating bearing of the wheel hub to the Michigan Scientific wheel force transducer. The hub adapter, wheel force transducer and the rim adapter – which holds the tire - from Michigan Scientific are mounted on top of the designed adapter. [2]

The capacity for the transducer was based on the guidelines given in SAE standards for force and moment testing and cleat testing:

Table 4: Estimation of Wheel Force Transducer Capacities

Force or Moment	Load Cell Capacity	
	Force and Moment Test	Cleat Test[3]
Longitudinal	0 to 18000 N	- (Maximum 100% Tire Load) $\leq F_X \leq$ (Maximum 100%

[2] Refer Appendix D for the details regarding tire wheel assembly

[3] The values are calculated based on an assumption that the machine is designed to test a tire with 100% load of 12500 N and a maximum loaded radius of 0.45 m.

Force		Tire Load) = ±12500 N
Lateral Force	±18000 N	- (Maximum 100% Tire Load) ≤ F_Y ≤ (Maximum 100% Tire Load) = ±12500 N
Normal Force	±900 N	- (300% Maximum Tire Load) ≤ F_Z ≤ 0 = -37500 N
Overturning Moment	±700 Nm	- F_Y Capacity Times Largest Loaded Radius ≤ M_Y ≤ F_Y Capacity Times Largest Loaded Radius = 5560 Nm
Aligning Moment	±700 Nm	- F_Y Capacity Times Largest Loaded Radius ≤ M_Z ≤ F_Y Capacity Times Largest Loaded Radius = 5560 Nm
Rolling Resistance Moment	±270 Nm	-

The force and moment measuring capacities for the wheel force transducer chosen for the machine have been listed in the table below:

Table 5: Wheel Force Transducer Capacity

F_X, F_Z	50000 N
F_Y	30000N
M_X, M_Y and M_Z	8100 Nm

3.1.3 Ball Screw: The ball screw is placed inside the box member and supported on both sides using roller bearings. The screw is not allowed to move along the axis of the box. As mentioned earlier, the force hub mount is fixed on the nut which travels over the screw. This helps in moving the force hub mount along the axis of the box. The ball screw is rotated using a DC motor from Maxon Precision Motors. The rotation of the ball screw will move the force hub mount along the axis of the screw and thus help in positioning the tire radially with respect to the drum.

3.1.4 Box Assembly: The basic purpose of using the box member in the design is to provide some structural stiffness to the tire positioning mechanism against the lateral force acting on the tire. The ball screw is mounted inside the box so that the lateral force from the force hub mount will be transmitted to the box as well as the ball screw. Different simulations were run for the ball screw individually and for the combination of ball screw and the box for the maximum forces acting on the assembly. The deflections for only the ball screw were considerably high. The addition of the box – an added structural member – reduced those deflections and stress values to acceptable levels.

The arrangement of the ball screw and the front box is shown in fig. 15.

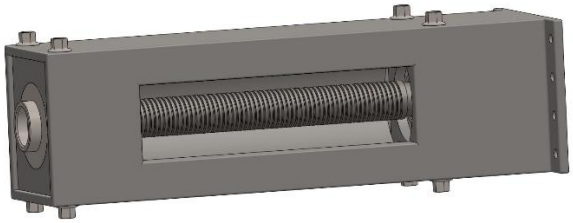

Figure 15: Front Box Assembly

3.1.5 Lateral Beam Member: A lateral beam is used in the design to join the box member in the front to the box member at the back. The basic function of this beam is to center the slip angle about the tire contact patch. This lateral member helps take out the offset induced by the box assembly (which is mounted offset to accommodate the tire width and force hub such that the tire contacts the drum at the center in the lateral direction). If the slip angle change is done in an offset position, the tire will ride up and down on the surface of the drum, bringing discrepancies to the measured data.

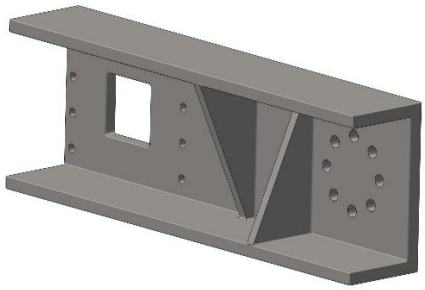

Figure 16: Beam

3.1.6 Spline Gearbox: The spline gearbox is used to connect the rear part of the box to the front part with the help of the lateral beam. The main function of this gearbox is to help achieve the slip angle change for the tire. The output flange of the gearbox is bolted to the beam in such a manner that the rotational output from the gearbox would be transmitted to the front box to be able to change the slip angle. The gearbox is driven using a motor and a planetary gearhead. The mechanism is designed to obtain a slip angle change of ±15°. The mechanism is capable of providing a sweeping slip angle change with a maximum frequency of 2.7 Hz.

3.1.7 Rear Box: The rear box member is bolted to the input flange of the spline gearbox. The motor and the gearhead used to drive the spline gearbox is fitted inside the box. The box is sandwiched between two plates and helps hold them in place.

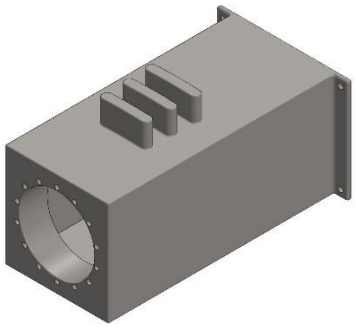

Figure 17: Rear Box Member

3.1.8 Supporting Plates: The rear box member is supported between two plates which restrict the motion of the box in the vertical plane. The interface between the box

and the plates is used for the camber angle change of the mechanism. The box has projections on it which can match up with the slots on the plates. The detail of this is shown in fig 18. The slots in the plate are designed such that a camber angle change of ±10° can be obtained. An electric linear actuator is used to apply a sideways force on the assembly which can make the box move in a constant radius arc about the tire contact patch – which acts as a pivot. The load bearing capacity of the actuator was estimated based on the maximum forces acting on the tire and the estimated values were validated using a simulation run in Abaqus CAE. The results of which are shown in fig 19.

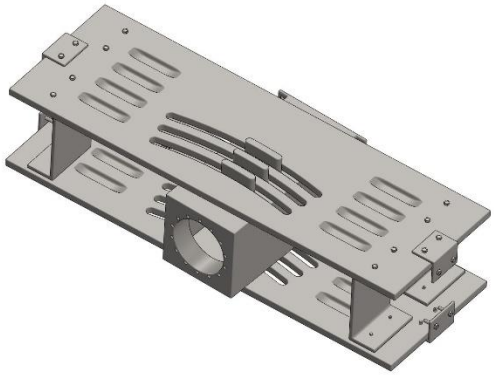

Figure 18: Rear Box and Supporting Plates Assembly

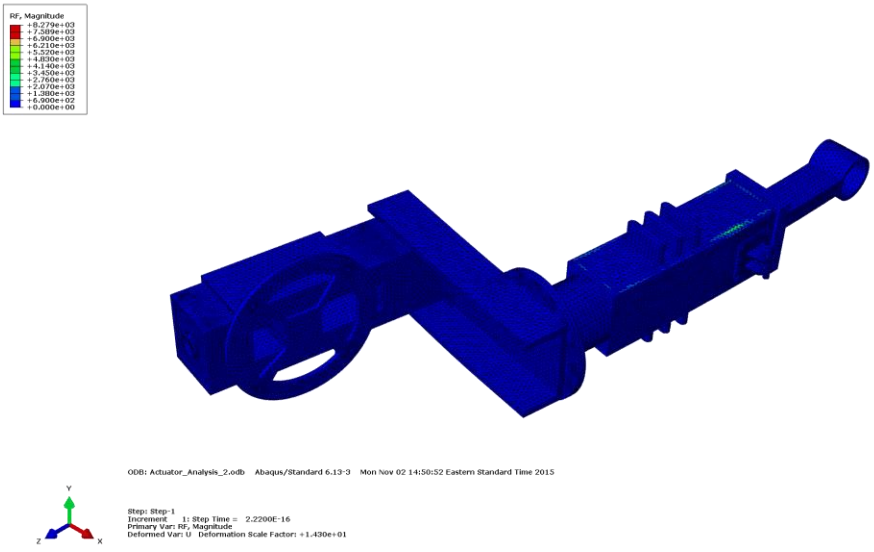

Figure 19: Loading Capacity - Camber Angle Change Actuator

The maximum force acting on the actuator was estimated in Abaqus CAE for the maximum amount of lateral and longitudinal force on tire. The maximum reaction force obtained by running the simulation was found to be 8279 N. An actuator with a load capacity of 13000 N is used in the design.

3.1.9 Reaction Rod Collar, Reaction Rod and Truss Members: The back end of the box is attached to a reaction rod collar which is free to slide over a reaction rod. The reaction rod collar stays in constant contact with the reaction rod with the help of spring loaded rollers which have been mounted inside the collar such that uniform contact is achieved. The reaction rod is welded on both ends to plates which are a part of the truss structure. The two main functions of this truss structure are: (a) to provide structural rigidity to the assembly especially against the forces arising due to cleat tests. (b) This truss structure provides a better way of applying a distributed normal force from the loading mechanism on the tire. The reaction rod collar is designed to sustain the bending and buckling forces. The reaction rod has a profile similar to the slots in the supporting plates. This reaction rod is designed to sustain the bending and shear forces.

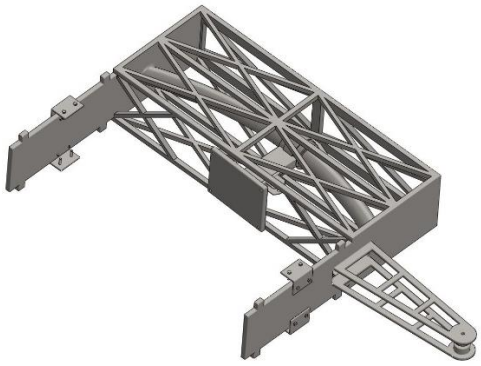

Figure 20: Reaction Rod Collar, Reaction Rod and Truss Members

The whole assembly for the tire positioning mechanism consisting of the components mentioned above is supported on linear bearings bolted to the machine

base and adjusted to a height where the tire will touch the drum at a point of maximum diameter.

3.2 Effect of Gyroscopic Moments

Gyroscopic effects are observed in a system, when an axis about which an object is spinning at a constant speed is also turning about another axis at a steady rate. Gyroscopic effects are observed in a lot of systems. These effects are also observed in automobiles because we have a tire rotating at a constant speed which gives rise to gyroscopic moments under steering effects or camber effects. Similarly, in the tire testing machine, the tire is spinning at a constant speed and the tire positioning mechanism is going to be used to obtain slip and camber angle change of the tire. Thus, the combined effect of the spinning of the tire and precessing about the slip angle axis and the camber angle axis is going to give rise to gyroscopic moments. These moments need to be taken into consideration while designing the mechanism.

The gyroscopic moments acting along the principal axes of inertia for a rigid body are obtained using Euler's equations and are given as follows [21]:

$$\sum M_x = I_{xx}\dot{\omega}_x - (I_{yy} - I_{zz})\omega_y\omega_z \quad (1)$$

$$\sum M_y = I_{yy}\dot{\omega}_y - (I_{zz} - I_{xx})\omega_z\omega_x \quad (2)$$

$$\sum M_z = I_{zz}\dot{\omega}_z - (I_{xx} - I_{yy})\omega_x\omega_y \quad (3)$$

Gyroscopic moments in the testing machine:

As the tire rotates at a constant speed on the tire positioning mechanism, the following gyroscopic moments arise in the system:

1. Gyroscopic moment due to camber angle change
2. Gyroscopic moment due to slip angle change

Calculations:

Assume that the tire mounted on the machine is rotating about X-axis. The Y- axis points upwards and the Z-axis is along the axis of the box or normal the contact patch. This tire orientation is shown in the figure below:

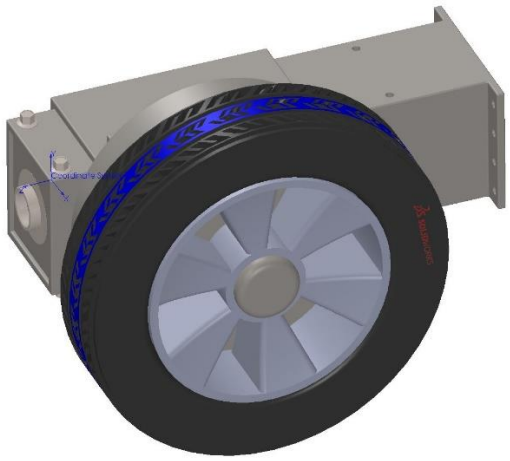

Figure 21: Tire Orientation

The speed of the tire was assumed to be 65 mph and the frequency for the camber and slip angle change was considered to be 4 Hz.

The values of moment of inertia along the three axes are

$$I_{xx} = 1.9207 \text{ kgm}^2$$

$$I_{yy} = 2.2931 \text{ kgm}^2 \quad (4)$$

$$I_{zz} = 2.2978 \text{ kgm}^2$$

The angular velocities about the three axes were taken as

$$\omega_x = \omega_{tire} = 110 \text{ rad/s}$$

$$\omega_y = \omega_{camber} = 2.792 \text{ rad/s} \quad (5)$$

$$\omega_z = \omega_{slip} = 4.188 \text{ rad/s}$$

3.2.1 Gyroscopic moment due to camber angle change

When the tire is undergoing a camber angle change, we have the tire spinning about the X-axis (spin axis) and additionally, because of the camber angle change, we also have a rotation about the Y-axis (precession axis). These two motions combined together will give us a moment about the Z-axis (torque axis).

Thus, the moment is obtained as follows:

$$\sum M_z = I_{zz}\dot{\omega}_z - (I_{xx} - I_{yy})\omega_x\omega_y$$

$$\sum M_z = -(1.9207 - 2.2931) \times 110 \times 2.792$$

$$\sum M_z = 114.38 \text{ Nm} \quad (6)$$

3.2.2 Gyroscopic moment due to slip angle change

Similar to camber angle change, when the tire is undergoing a slip angle change, we get a moment about the Y-axis. Thus, for a changing slip angle, X-axis is still the spin axis, Z-axis is the precession axis and Y-axis is the torque axis.

The magnitude of the moment is-

$$\sum M_y = I_{yy}\dot{\omega}_y - (I_{zz} - I_{xx})\omega_z\omega_x$$

$$\sum M_y = -(2.2978 - 1.9207) \times 4.188 \times 110$$

$$\sum M_y = 173.75 \text{ Nm} \quad (7)$$

3.3 Design of Loading Mechanism

Tire testing needs to be done at numerous normal loads. The machine being redesigned used a dead weight lever system originally for the application of normal load on tires. The dead weight loading systems tend to be less accurate, extremely

cumbersome and do not have the capability of being automated. Few other loading mechanisms which have been widely used in the past are: servo controlled hydraulic, pneumatic and servo controlled mechanical screw mechanisms. Hydraulic systems have large downtimes and prove to be quite problematic from the maintenance perspective. Motor driven mechanical screws have high loading capacities but they tend to have a sluggish response. Stiebel, Bine and Lyngsgaard (1980); found that servo controlled systems show a lot of variation in the applied load because of the flexible nature of the tire which gives rise to a continuous 'hunting tendency' of the servo valve to match the set point [22]. Another option which was taken into consideration was a pneumatic loading mechanism because it is less bulky, has less downtime, minimal maintenance requirements and because of the ability of a pneumatic system to respond faster. After a discussion with some experts, it was found that a pneumatic loading won't be sufficiently rigid for conducting cleat tests on tires because of the large forces generated in the normal direction after a tire passes over a cleat. Since, the tire passes over the cleat in every rotation of the drum, there would be continuous vibrations in the loading mechanism. This makes it difficult to take accurate measurements and makes maintaining a constant vertical load on the tire challenging.

Comparing the pros and cons for the options discussed above, a loading mechanism consisting of an electromechanical screw was designed to apply loads up to 25000 N on the tire. The maximum loading capacity for the mechanism was decided based on the guideline mentioned in standard for cleat testing, SAE J2730, which specifies it to be nearly twice the 100% load capacity for the tire to be tested.

The proposed loading mechanism consists of the following components: lead screw, AC motor and a worm gearbox.

The schematic representation of the loading mechanism is as follows:

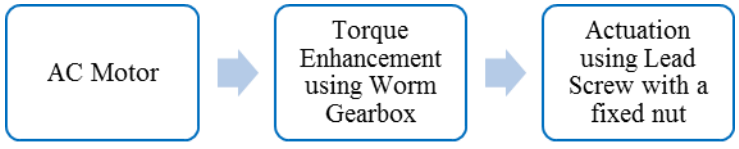

Working: The loading mechanism is driven with the help of an AC motor having a rating of 1 HP and 1440 rpm. The output of this motor is connected to a worm gearbox having a reduction ratio of 40. This worm gearbox gives sufficient increase in the torque of the motor to drive the loading mechanism with the requisite force. The output of the worm gearbox is connected to the lead screw with the help of universal joint. The nut of the lead screw is fixed on a bracket and the screw is free to move. As the screw is driven, the motion is transmitted to the truss structure (from the tire positioning mechanism) in the front so as to apply the requisite force on the tire. The lead screw is attached to the truss member using a ball joint. The motor and the worm gearbox are placed on sliding rails so that both of them can move with the screw.

The overall assembly of the machine, the tire positioning mechanism and the loading mechanism is shown below:

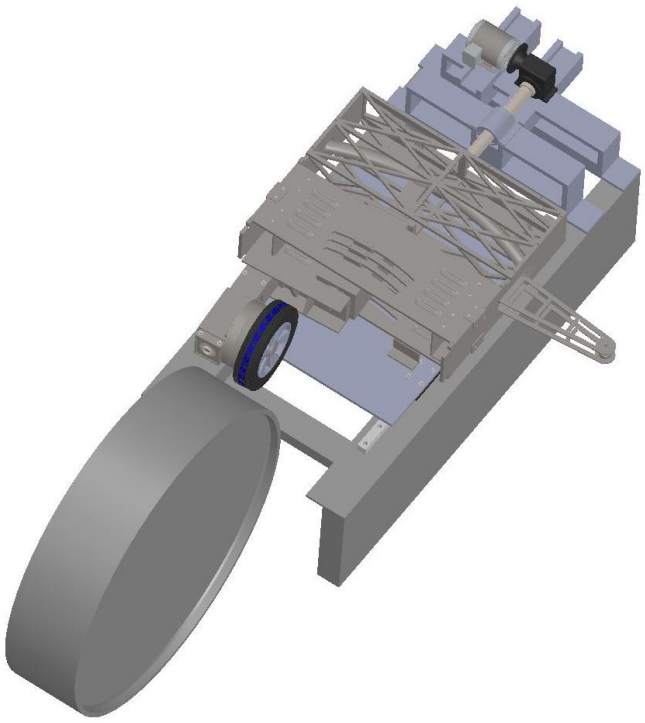

Figure 22: Complete Assembly

3.4 Overall Functioning of Machine

The tire positioning mechanism is going to be supported on the linear bearings mounted on the machine base with the help of a supporting plate. The tire positioning mechanism can traverse along the length of the linear bearings which helps in accommodating tires of different sizes. Suitable brackets are used to mount the tire positioning mechanism so that the tire will touch the drum at a point of maximum diameter. The loading mechanism is mounted behind the tire positioning mechanism and is rigidly fixed to the machine base using brackets.

3.5 Vibration Isolation

Any heavy machinery cannot be directly installed on a concrete floor because there would be uneven contact between the machine and the floor which would further lead to alignment issues and non-uniform load transfer to the concrete floor. Most of the machines have heavy rotating parts which can be a cause of vibrations in the machine. These vibrations or impact loads from the machine are transmitted from the machine to the floor and ultimately to the building foundation. If these vibrations and forces are not damped out using suitable means, it could harm the stability of the foundation from the long term perspective.

One of the most common procedure is to put grout under the machine base to damp out the vibrations. For this, instead of resting the machine directly on the concrete floor, some clearance is kept between the two by supporting the machine on bolts. The area is then filled with grout having the required physical properties (appropriate compressive strength, bearing area, flow ability etc.).

A three component epoxy grout was put underneath the machine base to dampen the vibrations. Prior to that, the concrete floor was roughened using a hand-grinder to ensure a good bond between the grout and the floor. The gap between the base and the floor was closed using wood panels. The epoxy was mixed as per instructions and was poured in the gap. The grout was cured at nearly 70° F for 24 hours for it to set properly.

Figure 23: Grouting of the Machine

3.6 Road Simulation

The rolling resistance machine had an 80 grit sand paper on the drum for testing purposes. This sand paper was removed using proper techniques and the drum is left bare for now. The drum would be covered with sand paper or any other required surface to simulate the conditions the testing needs to be done on.

Figure 24: Sand Paper Removal

Figure 25: Drum Cleaning the Adhesive using Citrus Stripper

Figure 26: Drum Surface Cleaning using Acetone

3.7 Tire Pressure

The tire pressure is one of the critical components affecting the forces and moments generated by the tire. Since, the tire heats up after running for a while, the pressure inside the tire increases as well. Thus, the tire pressure needs to be monitored throughout the test. In the design, the air pressure in the tire is going to be controlled using a rotary union connected to an air supply capable of maintaining the supply up to 120 psi.

CHAPTER 4: Finite Element Analysis of Design

This chapter talks about the structural and vibrational finite element analysis of a tire testing machine. The machine was designed to conduct force and moment test, rolling resistance test and cleat test on tires. The structural requirements of the tire positioning mechanism being different for each test, the structure was analyzed for maximum forces and moments acting on the assembly. Cleat testing subjects the tire as well as the structure to an impulse force which calls for the vibrational analysis of the assembly to avoid the structure from resonating. This chapter will focus on the static structural, modal and modal dynamic analysis for the designed machine.

The strength and the rigidity of the structure was estimated using finite element analysis. Static structural analysis was done for every part designed to estimate the maximum stress and deformation values. Critical stress regions were also taken a look at. Additionally, modal analysis was done for individual components of the assembly. Distinct frames of the assembly were also analyzed from the modal perspective to check if the structure is safe for the required frequency range. Additionally the entire assembly was analyzed to find out the structural frequencies when the components are assembled together on the machine. Modal dynamic analysis was carried out for the individual components, wherein a sinusoidal force profile representative of the forces acting on the structure when the tire passes over the cleat was applied to see the critical stress regions and to find out the maximum stress values generated in the structure.

4.1 Static Structural Analysis

The individual members of the assembly designed in-house were analyzed in Abaqus CAE to check for factor of safety under Von Mises stress and for maximum deformation. The parts modeled using Solidworks were imported into Abaqus CAE as STEP files for further analysis. The material used was 1018 Carbon Steel for most of the parts of the assembly except the tire-wheel assembly adapter, which was manufactured using 6061 Aluminum. The boundary conditions for the individual components were applied according to the constraints on the part in the actual assembly. The loads were applied as pressure and surface traction on the faces where

they are supposed to act in the assembly. The pressures and surface tractions were calculated based on the assumption that the maximum normal force acting on the tire is 25000 N and the maximum lateral force is 12500 N. The element used for meshing was C3D10 (10 node quadratic tetrahedron).

Table 6: Material Properties Used for Analysis

Material	Density (kg/m^3)	Young's Modulus (N/m^2)	Poisson's Ratio
1018 Carbon Steel	7900	2e11	0.29
6061 Aluminum	2700	6.9e10	0.33

The meshed model and the static analysis results for one of the parts of tire positioning mechanism have been shown in figure 23.

For this part, the normal force on tire was applied as pressure (3 MPa) and the lateral force was applied as surface traction (1.5 MPa) on an area where the force is going to be transmitted on the arched member welded between two plates. The number of elements in the meshed model were 1326392.

The maximum stress observed in the member was 33.3 MPa and the maximum deformation was 0.045 mm, which is well below the required limits.

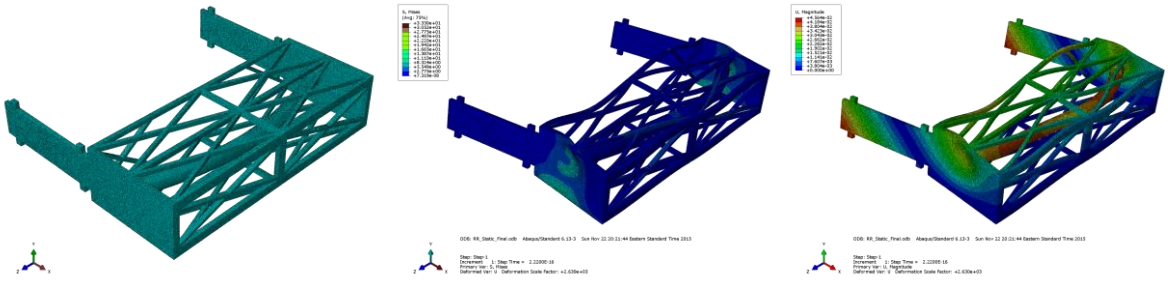

Figure 27: Meshed Model, Stress Contour and Deformation Contour for Reaction Rod

Similarly, all the critical components and individual assemblies in the design were tested for maximum loading.

The following table illustrates the Von Mises stress and deformation seen in individual components. The factor of safety is calculated based on a yield strength of 351 MPa for carbon steel and 276 MPa for aluminum. The allowable maximum deformation was limited to 1 mm and the minimum required factor of safety was set at 2.5.

Table 7: Stress and Deformation Results for Individual Components of Assembly

Components	Number of Elements in the Meshed Model	Von Mises Stress (MPa)	Deformation (mm)	Factor of Safety Based on Von Mises Stress
Force Hub Mount	354922	41.72	0.0051	8.41
Front Box	380448	207.3	0.168	1.70
Front Box Assembly	598417	118.5	0.147	2.96
Beam	284643	175.0 (Stress concentration at points where boundary conditions are applied) 131.3 (Relevant value of maximum stress)	0.553	2.0 2.67
Supporting Plates	133945	58.84	0.176	5.96
Rear Box	364162	68.81	0.047	5.10
Reaction Rod	213830	113.5	0.202	3.09

Collar				
Reaction rod	1326392	33.3	0.045	10.54
Aluminum Adapter	84740	67.06	0.014	4.12

The deformation in all the components was found to be below the required threshold. Also, all the members except for front box and beam member had a factor of safety above 2.5. The box member when analyzed with additional structural members (box member assembly) showed lower stress values. For the beam member, the maximum stress was found in very few elements and was seen to result from the way the boundary conditions were applied. Thus, the maximum stress can be safely neglected. The critical stress region for the beam showed a stress value 131 MPa and hence a factor of safety of 2.67.

In addition to the individual components, the entire assembly was analyzed in Ansys Workbench for the loads and moments acting on the tire. The forces and moments were applied on the force hub mount. The stress and deformation plots for this loading have been shown below:

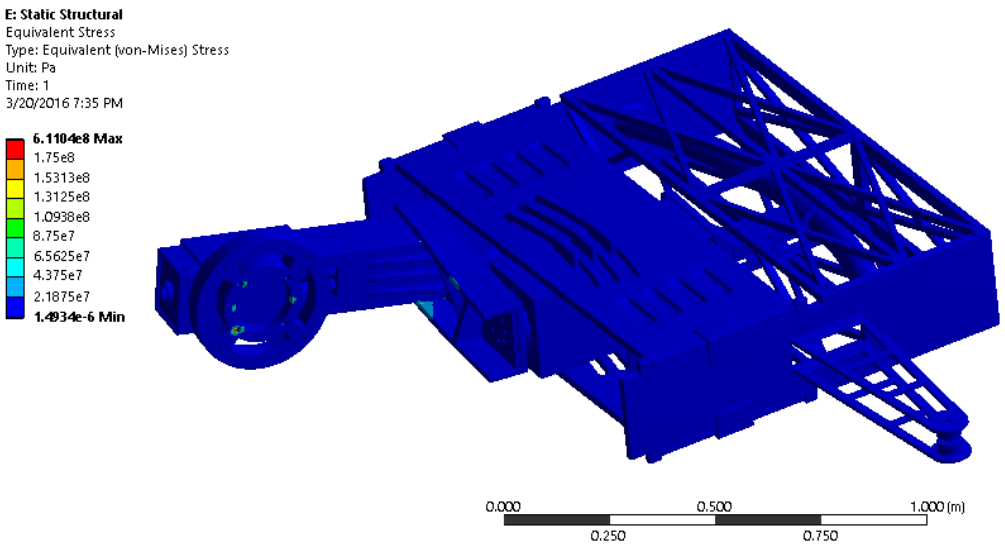

Figure 28: Stress Contour for Static Analysis of Tire Positioning Mechanism

The maximum stress was observed to be 611 MPa, but this was only in the region where the stress was concentrated because of the application of point forces for the moments. The maximum stress observed otherwise was 153 MPa which is well below the yield strength for the material. The magnified plot of stress concentration is shown below for reference:

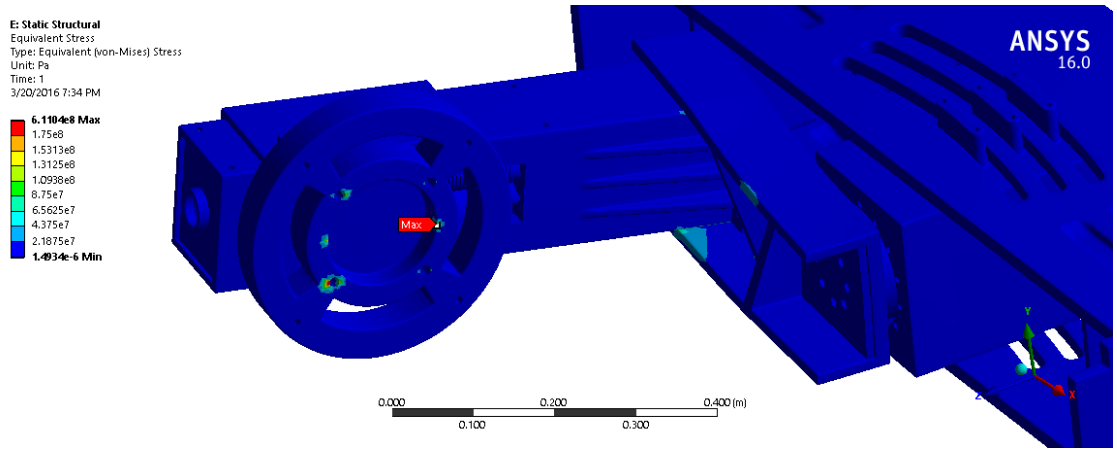

Figure 29: Magnified Stress Contour for Static Analysis of the Tire Positioning Mechanism

Similarly the deformation of the assembly for the applied loading was well below the decided limits i.e. 0.8 mm. The plot for deformation has been shown below:

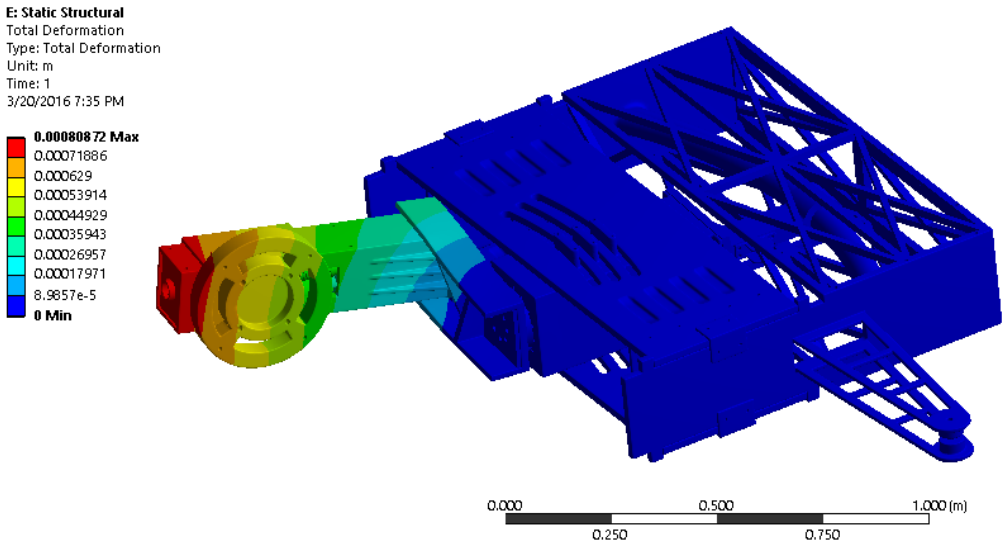

Figure 30: Deformation Contour for Static Analysis of the Tire Positioning Mechanism

4.2 Modal Analysis

The designed machine is going to be used to conduct cleat testing of tires. The test will include rolling the tire over a cleat (15X15 mm cross section) which is fixed either perpendicular or oblique to the direction of tire travel. This rigorous testing of tires subjects the machine to a large amount of vibrations and the machine needs to be designed to avoid any resonances in the structure. The testing machine needs to be analyzed by taking into consideration the attached tire and rim for the total mass and inertia of the heaviest structure in the assembly.

Instead of analyzing the entire tire positioning mechanism assembly as a whole, different substructures/frames making up the assembly were analyzed separately. Prior research suggests that resonance characteristics of the individual frames are superimposed to form the frequency response of the entire assembly [23]. The assembly was divided into two frames and the Eigen frequencies were obtained for them individually. The entire assembly was analyzed separately to check for the Eigen frequencies of the entire structure. The bearings in the assembly were modeled as spring elements to obtain more realistic results.

The basic frequency for the machine was taken to be 7 Hz based on a maximum speed of 80 mph of the flywheel. The modal frequencies for the individual frames were considered safe for a value above 70 Hz (more than ten times the basic frequency of the machine).

The two parts of the tire positioning mechanism analyzed separately are denoted as frame 1 and frame 2 in the figure below:

The solid models for the frames were created using Solidworks and were imported into Ansys Workbench in a STEP file format. The frames were meshed using ‘SOLID187’ (3D, 10 node) and ‘SOLID186’ (3D, 20 node) element in Ansys Workbench.

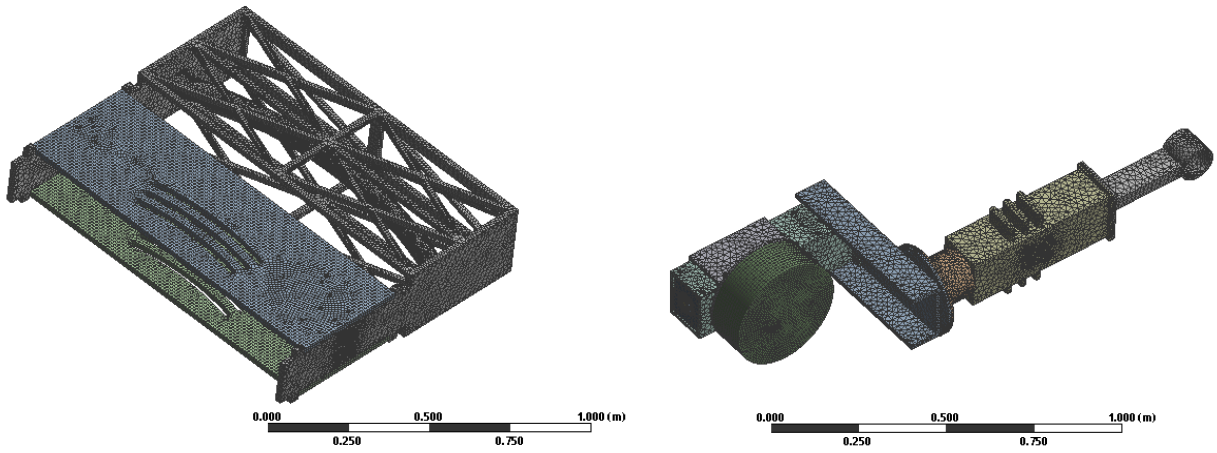

Figure 31: Meshed Model for Frame 1 and Frame 2

The results obtained for frame 1 and frame 2 are tabulated below:

Table 8: Modal Frequencies for Frame 1 and Frame 2, Iteration 1

Mode No.	Modal Frequency (Hz)	
	Frame 1	Frame 2
1	65.62	53.46
2	76.53	80.27
3	79.57	96.40
4	83.62	136.82
5	102.27	156.59
6	141.3	209.54
7	147.96	222.86
8	164.4	273.68
9	167.19	275.25
10	177.4	355.22

For frame 1, a mode at a frequency of 65 Hz was observed. The deformation for this mode is shown in the plot below:

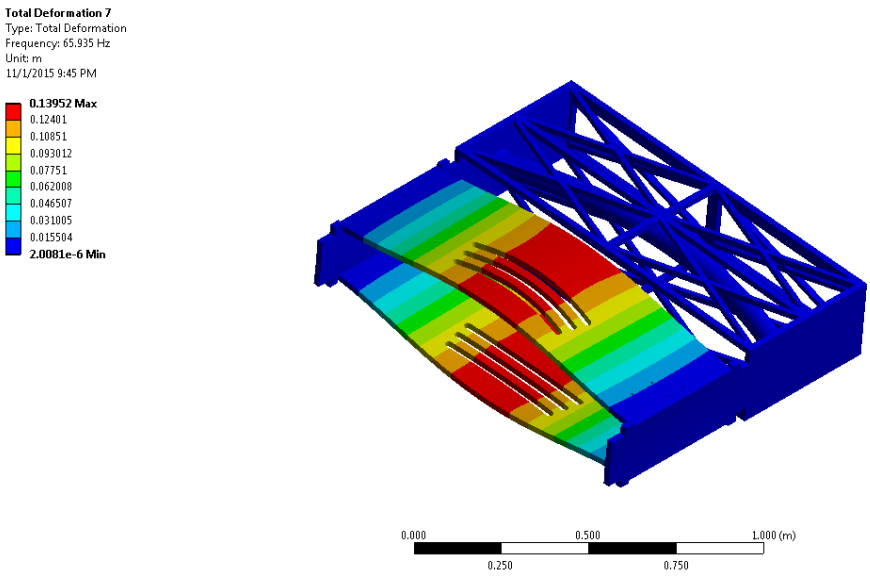

Figure 32: Deformation Contour for Frame 1, Modal Frequency = 65 Hz

The structure of the frame was modified to eliminate this mode and to bring up the modal frequency above 70 Hz. Some stiffeners were added on the plate and additional brackets were placed between the two plates to provide added rigidity to the structure. The results for the modified design have been listed in table 3.

For frame 2, the initial modal results showed considerable deformation in a few members for a frequency of 53.5 Hz. These modes were eliminated by adding stiffeners to the deformed members. The deformation plot for frame 2 at a frequency of 53.5 Hz is shown in figure 33.

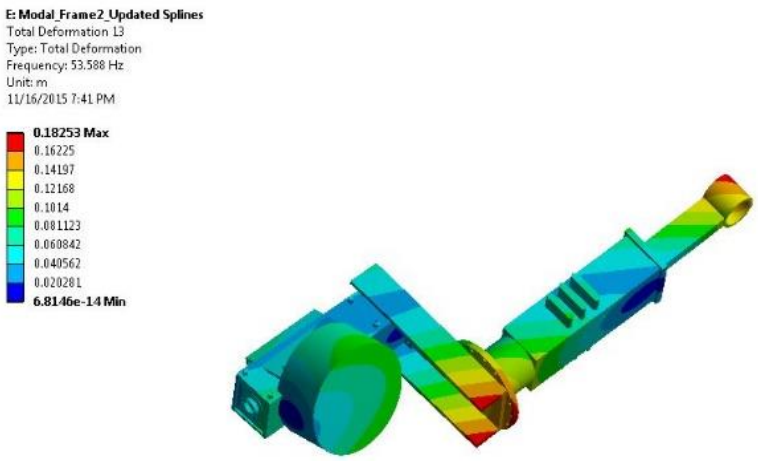

Figure 33: Deformation Contour for Frame 2, Modal Frequency = 53.5 Hz

The modal results for the modified design have been shown in table 9. The modal frequencies for the individual frames have been compared with the modal results for the entire assembly.

Table 9: Final Results for Modal Analysis of Frame 1 and Frame 2

Mode No.	Modal Frequency (Hz)		
	Frame 1	Frame 2	Complete Assembly
1	115.51	104.92	98.917
2	149.53	162.98	122.67
3	173.03	238.96	148.39
4	175.97	271.8	174.42
5	195.43	273.49	186.16
6	210.22	519.19	193.67
7	228.12	793.48	226.23
8	241.47	923.22	233.77
9	263.7	1006.4	252.59
10	286.91	1148.4	262.43

From the above table, we can see that the Eigen frequencies for the complete assembly are not an exact superposition of the Eigen frequencies obtained for individual subsystems/frames of the assembly. The difference observed in the frequencies is due to the lack of exact emulation of boundary conditions for individual frames as found in the complete assembly.

The first modal shapes for frame 1, frame 2 and the complete assembly are shown in the following figures:

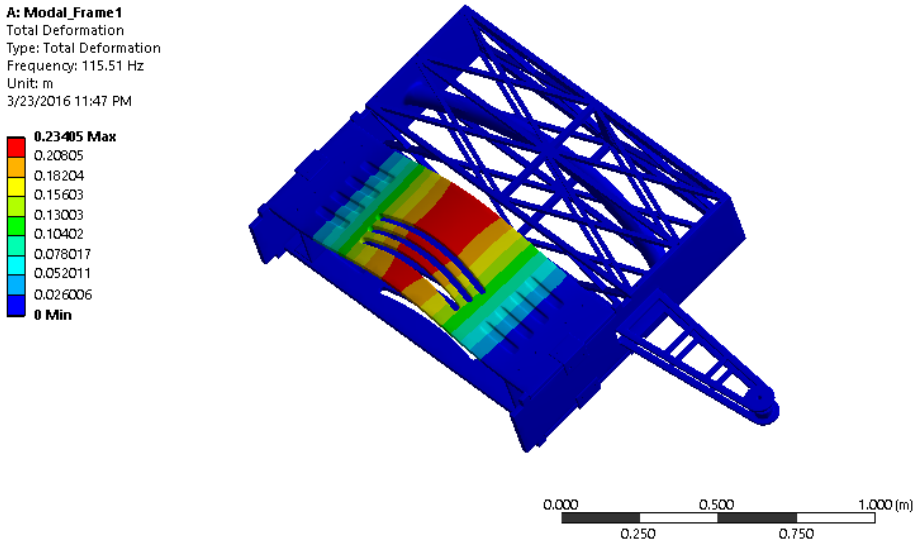

Figure 34: 1st Mode Shape for Frame 1 (Eigen Frequency = 115.51 Hz)

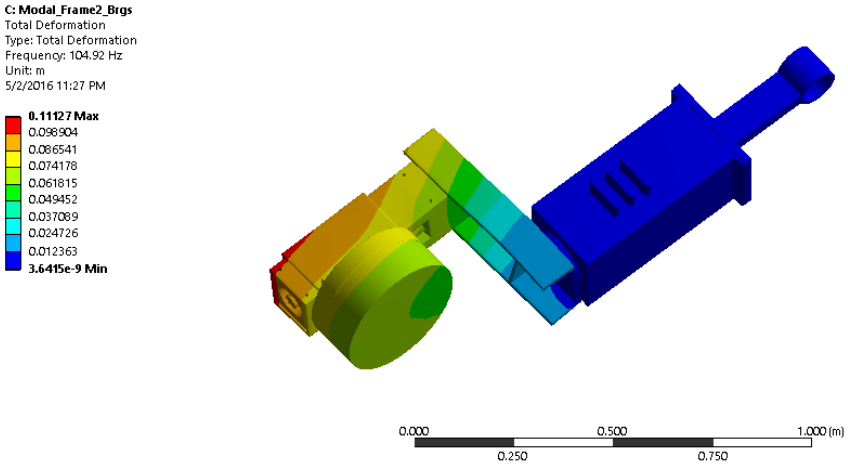

Figure 35: 1st Mode Shape for Frame 2 (Eigen Frequency = 104.9 Hz)

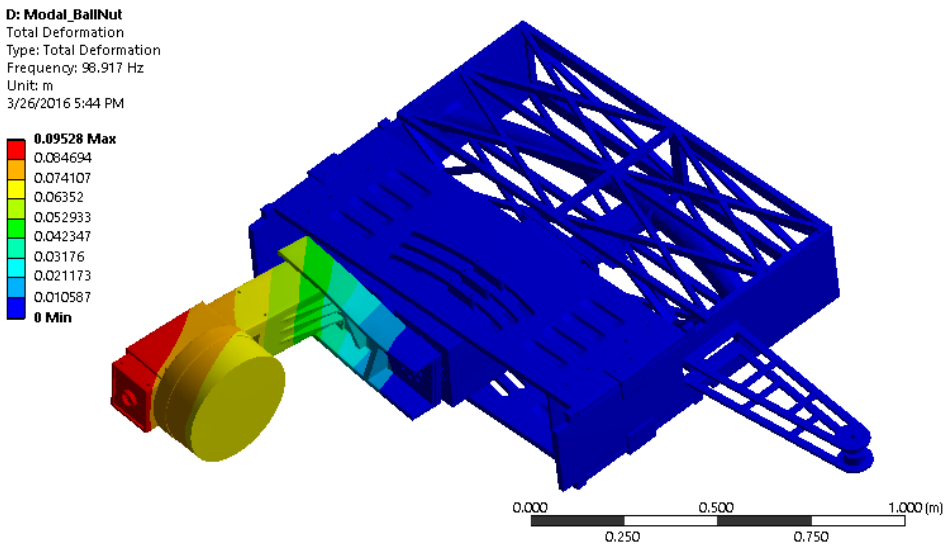

Figure 36: 1st Mode Shape for Tire Positioning Mechanism (Eigen Frequency = 98.91 Hz)

4.3 Modal Dynamic Analysis

Modal dynamic analysis was performed on the individual parts of the assembly to check the suitability under cleat test. The analysis was done using Abaqus CAE and the part creation and import into Abaqus CAE was done similar to static analysis. The boundary conditions were applied on individual components based on the way they are assembled on the machine. A sinusoidal load with a frequency of 7 Hz was applied on the components, the maximum amplitude of which was 25000 N for longitudinal force and 12500 N for lateral force.

The stress results for the time steps were studied to find the maximum value of stress and to locate the regions with high stress. The regions with high stress were kept unchanged while doing any changes from the manufacturing perspective.

The following figure shows how the stress varies in the reaction rod assembly for a time increments of 0.1 seconds. Also, Eigen frequencies generated in the output step before modal dynamic analysis for each individual part were taken a look at to check for resonance.

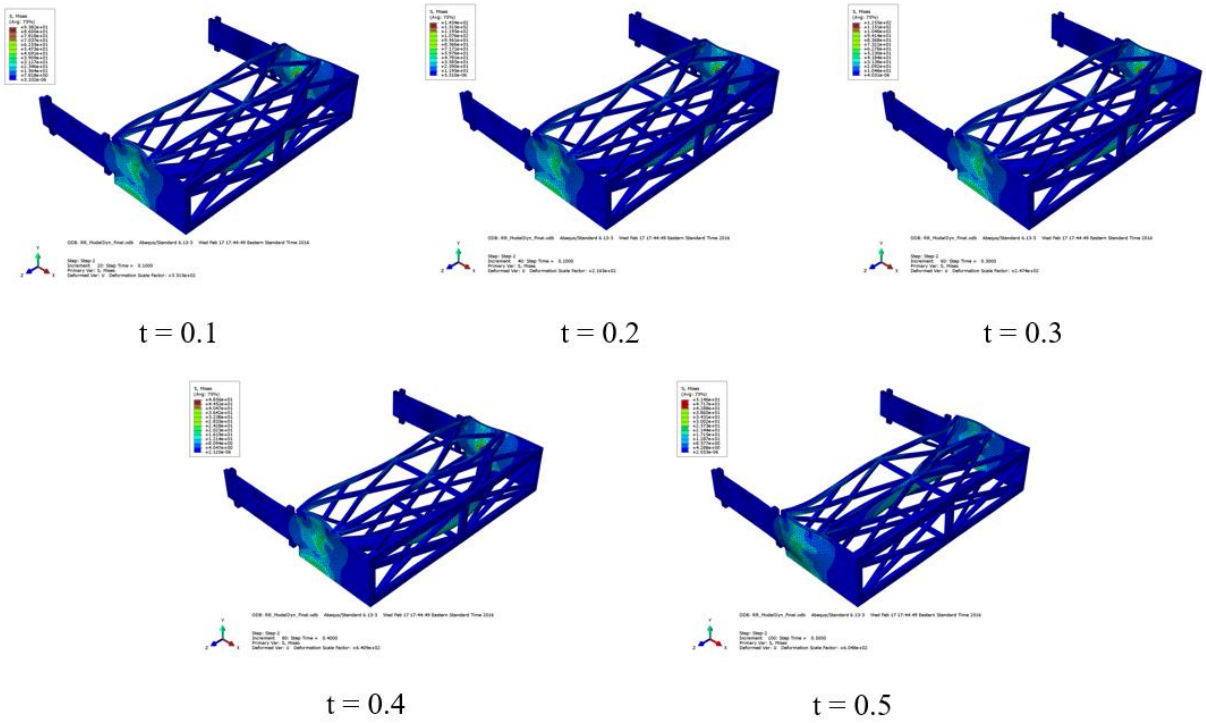

Figure 37: Modal Dynamic Analysis - Reaction Rod - Stress Contours at t = 0.1, 0.2, 0.3, 0.4, and 0.5 (Max. Value = 143.4 MPa)

Table 10: Eigen Frequencies for Reaction Rod

Mode	Frequency (Hz)
1	137.99
2	163.16
3	216.01
4	242.13
5	244.72
6	254.40
7	254.55
8	260.92
9	264.01
10	270.71

4.4 Limitations in Finite Element Analysis

- There is no way to estimate the validity of the results obtained from modal analysis since the machine has not been manufactured yet. Thus, it is possible that experimental modal analysis might give some different results as compared to the analytical FEA.

- Modal dynamic analysis was done using a critical damping fraction of zero, since, there were no experimental means available to estimate the actual damping of the structure.
- Being a huge structure, the meshing was mostly done using quadratic tetrahedrons instead of using other high quality elements (hex elements) to reduce the computational time. Thus, there might be some error in the stress and deformation values obtained in the analysis. But, the element size being sufficiently small, the error will not be of much significance.

CHAPTER 5: Design for Manufacture (DFM)

Design for Manufacture (DFM) is a concept which has become quite popular in the product design industry to optimize the design process. The design of a product is done taking into consideration the manufacturing perspective throughout its development phase. The design is changed in such a manner so as to reduce material costs, labor costs and overhead costs. Since, the design of this machine involves a lot of custom parts, most of them had to be manufactured using machining procedures instead of castings. Hence, the design was optimized based on two critical factors: tooling costs and machining time. The material costs were reduced by replacing a part machined out of single material billet with two parts then joined together using suitable means.

The following parts of the design were changed to make it easier for manufacturing and assembly:

5.1 Reaction rod collar

The reaction rod collar was initially designed to match the curvature of the rod in the reaction rod assembly. The friction was reduced by using bushings inside the collar. From making it easier to manufacture, the curvature of the collar was removed and the collar was made straight instead. The bushing was replaced by spring loaded bearings to rest the collar on the rod in the reaction rod assembly. Sufficient bearings were used to attain proper contact between the rod and the collar and also to sustain the loads acting on the assembly.

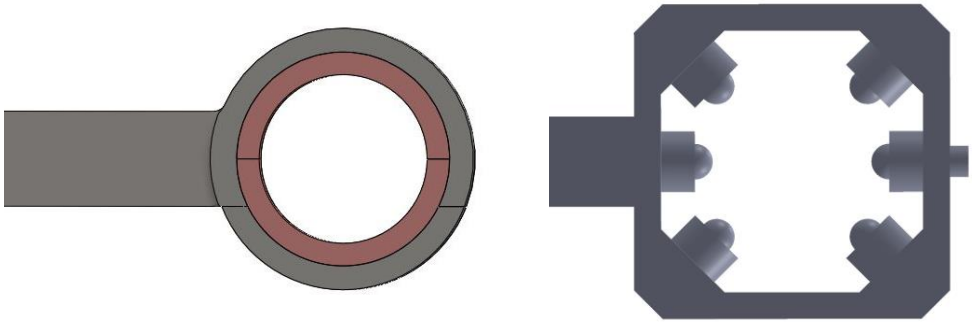

Figure 38: Change in Cross-Section of Collar

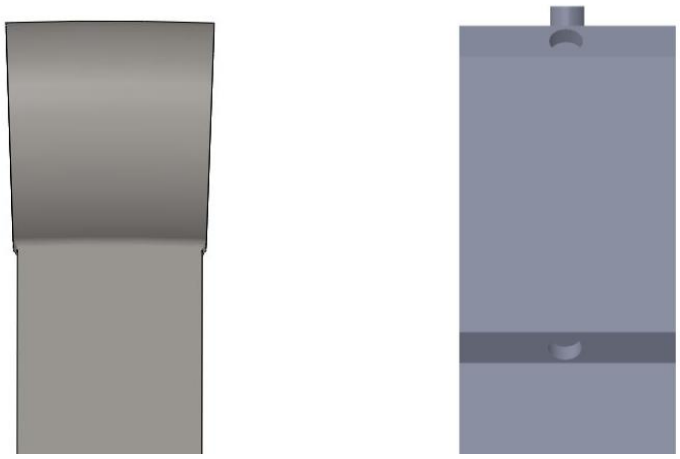

Figure 39: Change in Curvature of Collar (Top View)

5.2 Reaction rod assembly

The reaction rod assembly was manufactured from individual plates to speed up the manufacturing process. The individual plates were assembled together after cutting the required profiles in them. The reaction rod was welded between the two vertical plates positioned opposite to each other. Also, the rod in the assembly was initially designed to have a circular cross section. To achieve the required accuracy in the arc profile of the rod, the cross section was changed to a 70X70 mm cross section. The edges of the rod were rounded off such that the spring loaded bearings would rest on the rod.

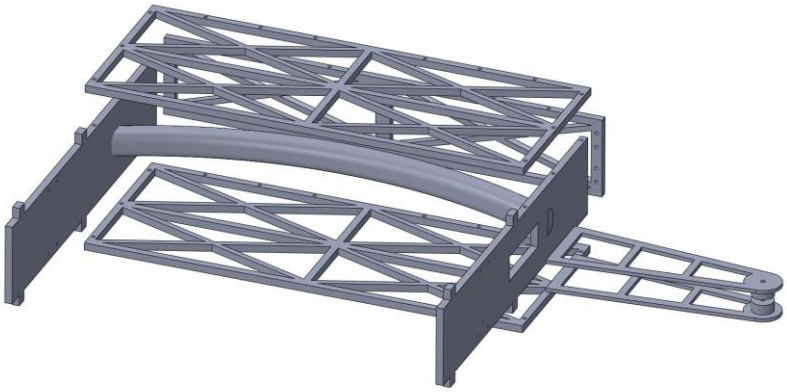

Figure 40: Reaction Rod Updated Assembly

5.3 Front box

The front box was designed to have a square cross section on the inside in the initial design. To reduce the machining time and cost, the inside cross section was made circular. Additional modifications were done to the box to accommodate the motor which drives the radial positioning screw. The assembly is shown in the picture below:

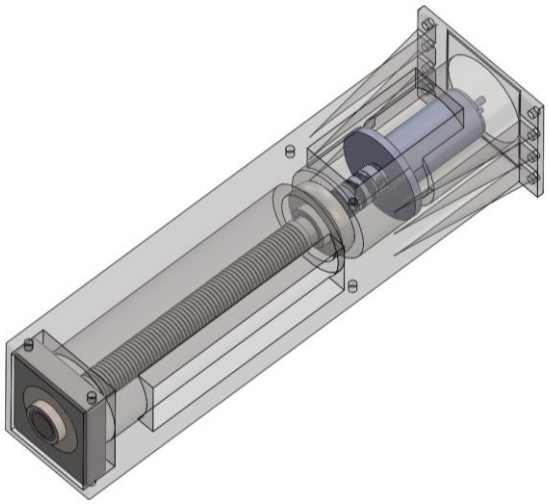

Figure 41: Front Box Assembly

5.4 Rear box

Similar to the front box, the inner cross section of the rear box was changed from square to circular. Instead of welding the fins on the box, they were positioned on the box with dowel pins and fastened using bolts. Appropriate provision was made to mount the motor driving the slip angle change gearbox. The motor shaft was connected to the gearbox input using a separately designed shaft coupling.

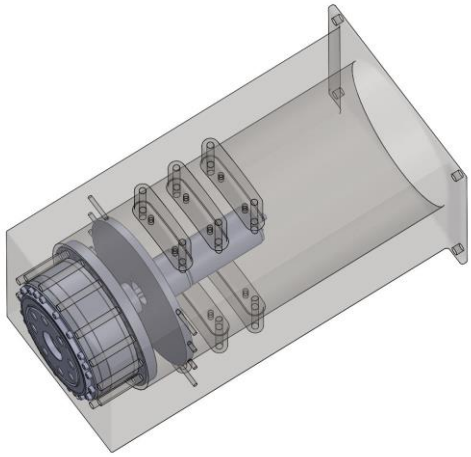

Figure 42: Rear Box Assembly

5.5 Force hub mount

The force hub mount was not manufactured using a single billet to make it easier to assemble on the front box assembly. The boss mounted on the nut of the radial positioning screw was machined separately, located using dowel pins and then bolted on the front flange of the force hub mount. The flanges of the force hub mount were bolted on the front face of the force hub mount in the end.

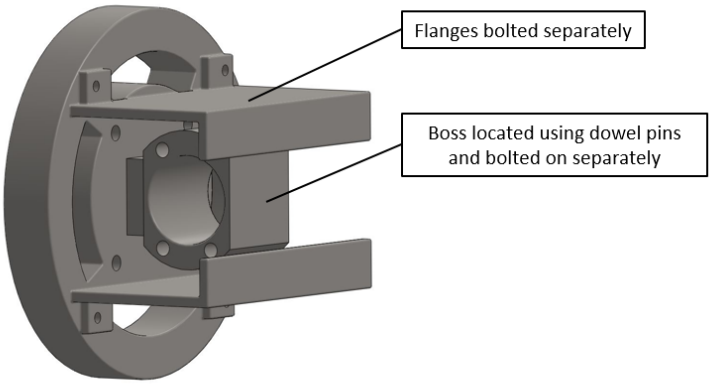

Figure 43: Force Hub Mount Assembly

CHAPTER 6: Conclusions and Future Work

6.1 Conclusions

The purpose of redesigning the rolling resistance machine was to be able to conduct various tests using a single setup. The force and moment test along with rolling resistance test and cleat test can be carried out using this design. The design is capable of accommodating passenger car tires and light truck tires. The machine was designed for slip angle sweep range of ±15° and the camber angle range is ±10°. An improved version of a loading mechanism was also designed to replace the previous one.

Some additional advantages of this design include the cost effectiveness of the design and its multipurpose functionality. Also, since the input parameters – slip angle, camber angle and the normal force are uncoupled, the design allows for various possibilities under which the tire can be tested.

The analysis helped identify the suitability of the machine for conducting heavy duty tire testing. The critical stress regions identified from the analysis were helpful in defining the approach for the manufacturing of the machine. The modal dynamic analysis helped identify the dynamic behavior of the individual components of the design under maximum loading. The modal analysis of the assembly and individual frames was done to avoid any resonance in the assembly during cleat testing. A few additional Eigen frequencies were found for the entire assembly as compared to the individual frames which could be a result of different boundary conditions.

The modal analysis can be validated by conducting experimental modal analysis once the machine has been manufactured and would also be helpful to get an estimate of the damping of the structure.

Some trivial and a few major changes had to be done to design to reduce the manufacturing costs. The primary factors taken into consideration for optimization of the design from the manufacturing perspective were – tooling cost, material cost and machining time. The changes made to the design were done such that the strength and rigidity of the mechanism was not compromised.

6.2 Discussion

Since, the machine was designed to carry out different tests, some parts of the design could not be narrowed down on. For instance, the road surface requirements for all the tests are different. Thus, conducting these tests back to back on the machine might be a problem if the road surface is not simulated according to appropriate guidelines in the standard. Also, the actuator used in the design for camber angle change is not capable of doing the camber angle change at high speeds. Thus, the tests will be carried out at discrete camber angles. The slip angle change is centered for a specific width of the tire. When conducting tests on different tires, there might be a possibility of an offset. This offset needs to be taken into account in the data acquisition software for that individual tire.

The entire design is validated using finite element analysis in Ansys Workbench and Abaqus CAE. There being a difference in the boundary conditions and loads applied in the simulation and the real behavior, there is a possibility of some error in the stress and deformation estimates obtained using FEA. The limitation in the modal dynamic analysis is the uncertainty of an exact value of damping in the structure because of lack of any experimental data.

6.3 Future Work

- After the fixture has been manufactured and assembled, the data obtained by carrying out different tests for tires needs to compared with the empirical results and some actual measurements need to be done to determine the accuracy of the machine. The data obtained for a particular tire needs to be compared with the data obtained using a similar tire testing machine. The repeatability of the data measured using the machine needs to be ascertained by using appropriate statistical methods.
- In future, several other tests can be conducted using the same setup and by doing a few minor changes to the design like tire noise testing, tire tread wear or tire footprint measurement.

Bibliography

[1] J. L. Ginn, R. F. Miller, R. L. Marlowe, and J. F. Heimovics, “The B. F. Goodrich Tire Dynamics Machine,” *SAE Tech. Pap. Ser.*, 1962.

[2] S. K. Clark and D. J. Schuring, “Interlaboratory Tests for Tire Rolling Resistance,” *SAE Tech. Pap. Ser.*, 1978.

[3] A. Bhoopalam and K. Kefauver, “Using Surface Texture Parameters to Relate Flat Belt Laboratory Traction Data to the Road,” *SAE Tech. Pap.*, 2015.

[4] A. W. Bull, “Tire Behavior in Steering,” *Soc. Automot. Eng. J.*, vol. 45, no. 2, pp. 344–350, 1939.

[5] J. R. Luchini, “Test surface curvature reduction factor for truck tire rolling resistance,” *SAE Tech. Pap. Ser.*, 1982.

[6] SAE International Surface Vehicle Recommended Practice J1107, “Laboratory Testing Machines and Procedures for Measuring the Steady State Force and Moment Properties of Passenger Car Tires,” *SAE Stand.*, 2012.

[7] V. E. Gough and S. G. Whitehall, “Universal Tyre Test Machine,” *FISITA Proc.*, pp. 117–137, 1962.

[8] D. L. Nordeen and A. D. Cortese, “Force and Moment Characteristics of Rolling Tires,” *Soc. Automot. Eng. Pap.*, pp. 325–336, 1963.

[9] J. L. Ginn, “Road Contact Forces of Truck Tires as Measured in the Laboratory,” *SAE Tech. Pap. Ser.*, 1967.

[10] D. Howard and B. J. Brown, “Measurement of Tire Shear Forces,” *SAE Tech. Pap. Ser.*, 1970.

[11] T. E. Ritter, “Design of Laboratory Equipment for Routine Tire Force Force and Moment Testing,” *SAE Tech. Pap. Ser.*, 1972.

[12] K. D. Bird, “The Calspan Tire Research Facility: Design, Development, and Initial Test Results,” *SAE Tech. Pap. Ser.*, 1973.

[13] W. J. Langer and G. R. Potts, “Development of a Flat Surface Tire Testing Machine,” *SAE Tech. Pap. Ser.*, 1980.

[14] S. E. Lloyd, “Development of a Flat Surface Tire Rolling Resistance Facility,” *SAE Tech. Pap. Ser.*, 1978.

[15] SAE International Surface Vehicle Recommended Practice J1269, “Rolling Resistance Measurement Procedure for Passenger Car, Light Truck , and Highway Truck and Bus Tires,” *SAE Stand.*, 2006.

[16] J. Y. Wong, *Theory of Ground Vehicles*, Third. John Wiley and Sons, Inc., 2001.

[17] W. F. Milliken and D. L. Milliken, *Race Car Vehicle Dynamics*. Society of Automotive Engineers, Inc., 1995.

[18] T. Takahashi, M. Hada, K. Oyama, and H. Sakai, “New Model of Tire Overturning Moment Characteristics and Analysis of Their Influence on Vehicle Rollover Behavior,” *Veh. Syst. Dyn.*, vol. 42, pp. 109–118, 2004.

[19] SAE International Surface Vehicle Recommended Practice J2730, “Dynamic Cleat Test with Perpendicular and Inclined Cleats,” *SAE Stand.*, 2013.

[20] SAE International Surface Vehicle Recommended Practice J1106, “Laboratory Testing Machines for Measuring the Steady State Force and Moment Properties of Passenger Car Tires,” *SAE Stand.*, 2012.

[21] J. L. Meriam and L. G. Kraige, *Engineering Mechanics DYNAMICS*, Fourth. John Wiley and Sons, Inc., 1998.

[22] A. Stiebel, K. L. Bine, and J. Lyngsgaard, “A New Approach to Load Regulation of Tire Endurance Testing Machines,” *SAE Tech. Pap. Ser.*, 1980.

[23] H. Dong, “Dynamic Characteristics of a Machine Tool At Working Positions in Operating Test,” in *ASME 2011 International Design Engineering Technical Conferences and Computers and Information in Engineering Conference*, 2011, vol. 1, pp. 457–466.

References not cited in this article:

[24] Clark Samuel K. (), “Mechanics of Pneumatic Tires”, U.S. Department of Transportation, National Highway Traffic Safety Administration, Chapter 8

[25] Budynas Richard G. and Nisbett J. Keith (), “Shigley’s Mechanical Engineering Design, McGraw-Hill Education

APPENDIX A: Results for Static Structural Finite Element Analysis

The results for static analysis of individual components of the assembly have been shown below.

A.1 Force Hub Mount:

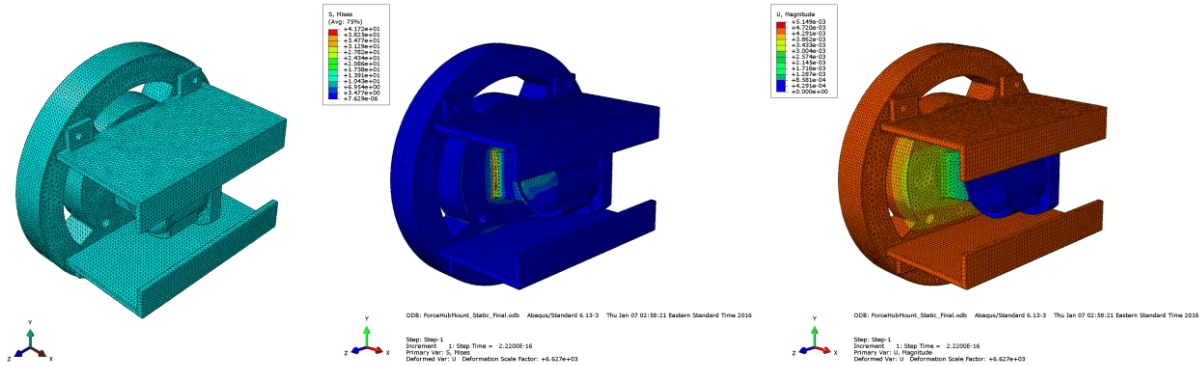

Figure 44: Meshed Model, Stress Contour and Deformation Contour for Force Hub Mount

A.2 Front Box:

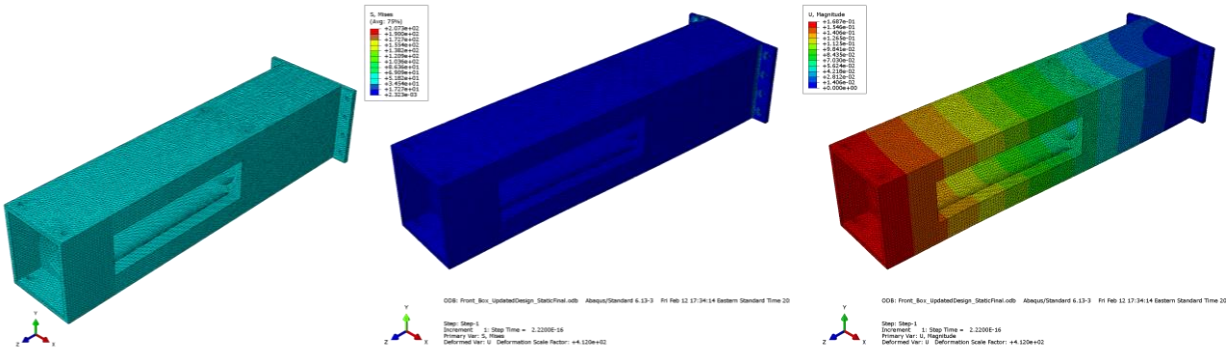

Figure 45: Meshed Model, Stress Contour and Deformation Contour for Front Box

A.3 Front Box Assembly:

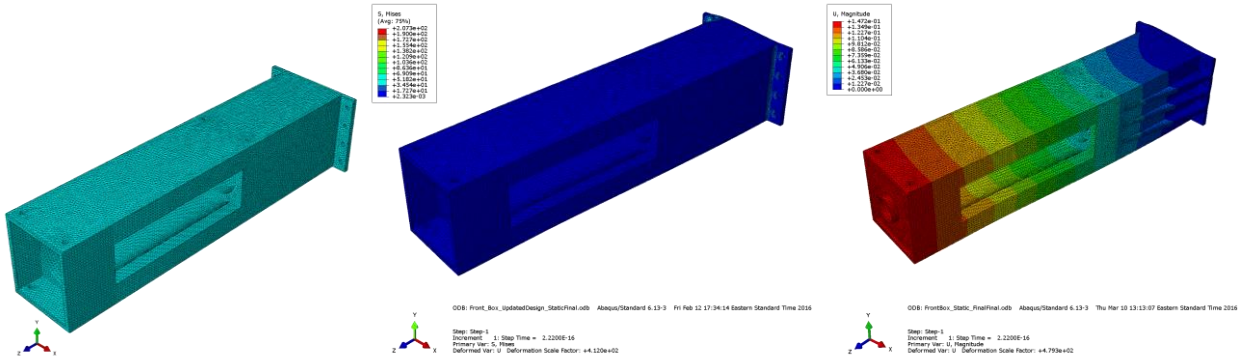

Figure 46: Meshed Model, Stress Contour and Deformation Contour for Front Box Assembly

The maximum stress value in the simulation for front box assembly was found to be more than the stress value in the box only. On investigating, it was seen that this value is only concentrated in a negligible area because of improper contact between two parts in the assembly.

A.4 Beam:

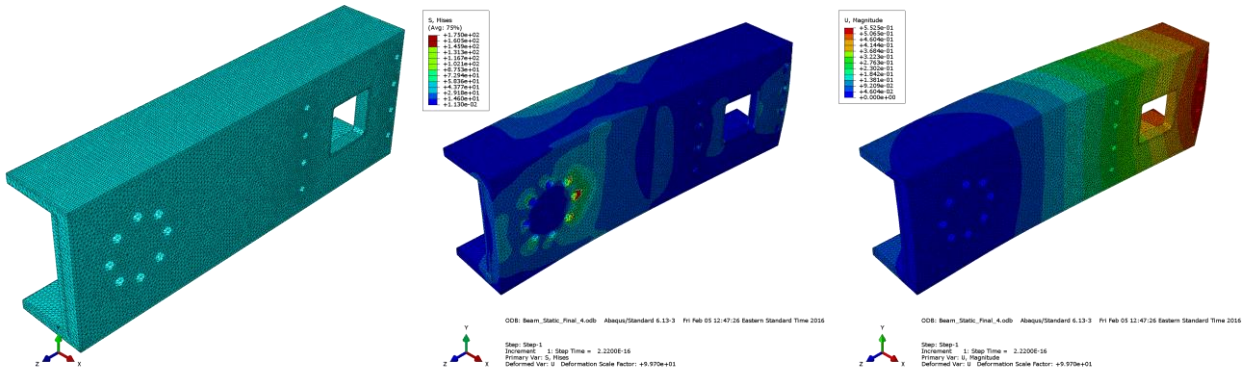

Figure 47: Meshed Model, Stress Contour and Deformation Contour for Beam

A.5 Supporting Plates:

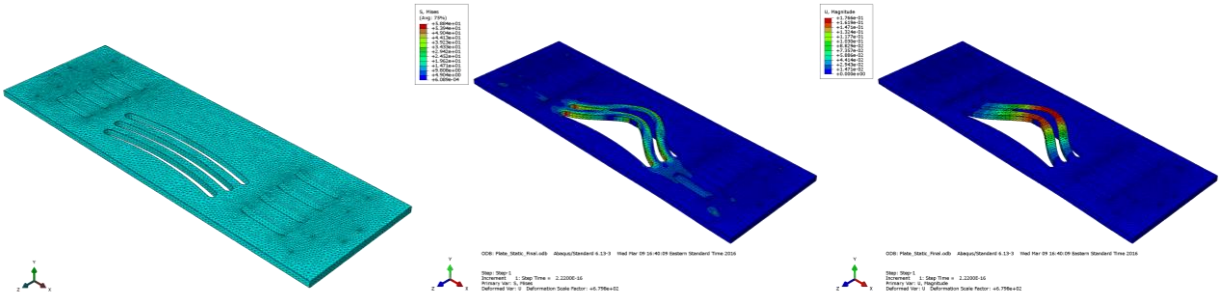

Figure 48: Meshed Model, Stress Contour and Deformation Contour for Supporting Plates

A.6 Rear Box:

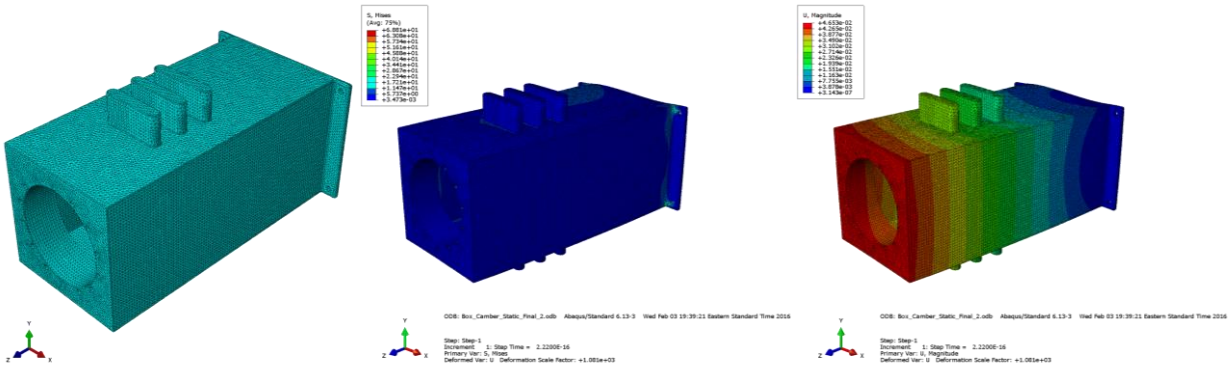

Figure 49: Meshed Model, Stress Contour and Deformation Contour for Rear Box

A.7 Reaction Rod Collar:

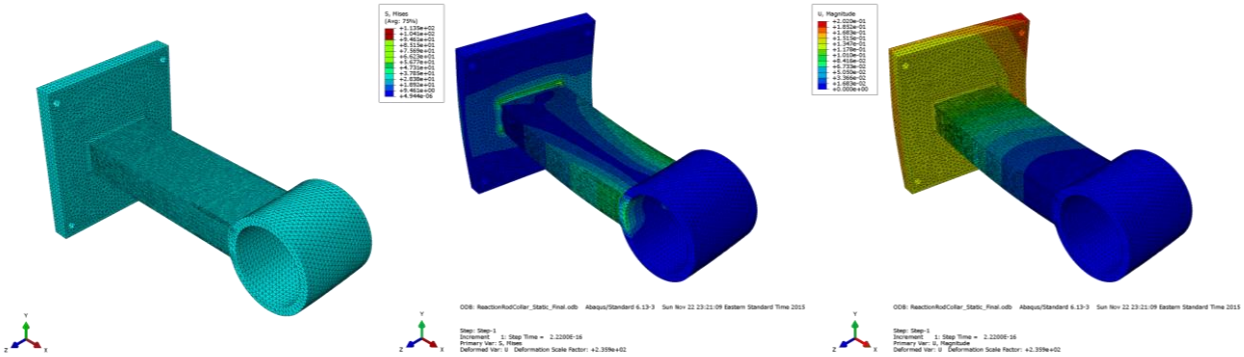

Figure 50: Meshed Model, Stress Contour and Deformation Contour for Reaction Rod Collar

A.8 Aluminum Adapter:

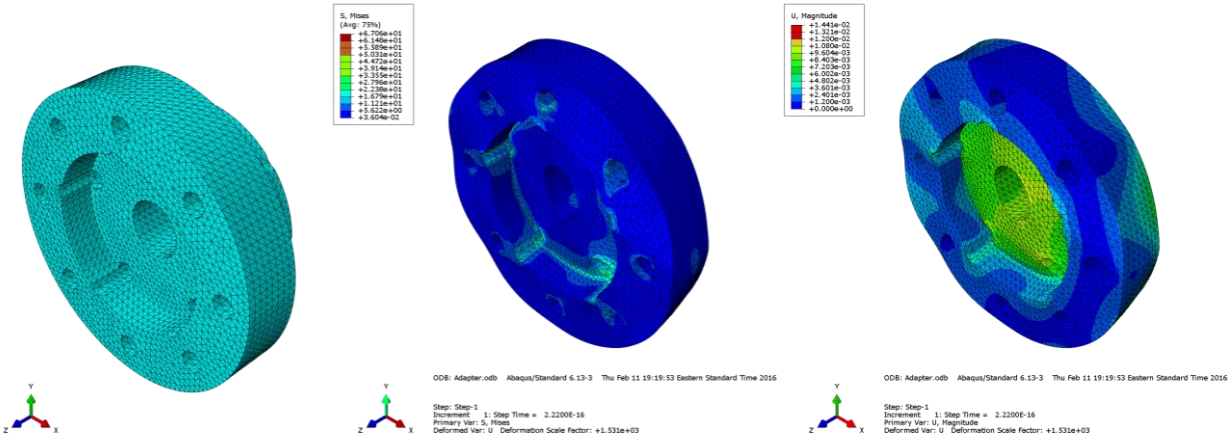

Figure 51: Meshed Model, Stress Contour and Deformation Contour for Aluminum Adapter

A.9 Reaction Rod Actuator Force Response

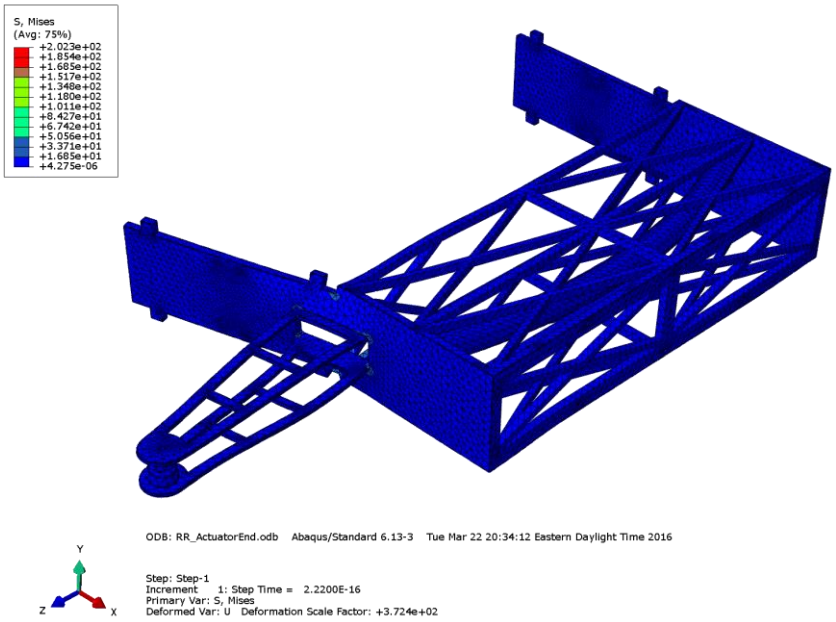

Figure 52: Stress Contour on Reaction Rod for Actuator Force (Maximum Value = 202.3 MPa)

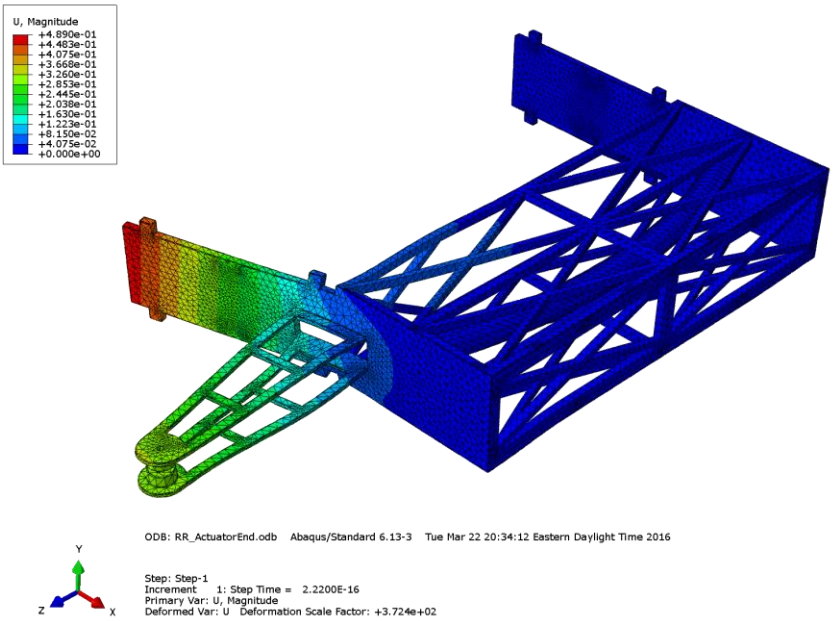

Figure 53: Deformation Contour on Reaction Rod for Actuator Force (Maximum Value = 0.489 mm)

APPENDIX B: Results for Modal Dynamic Finite Element Analysis

B.1 Force Hub Mount:

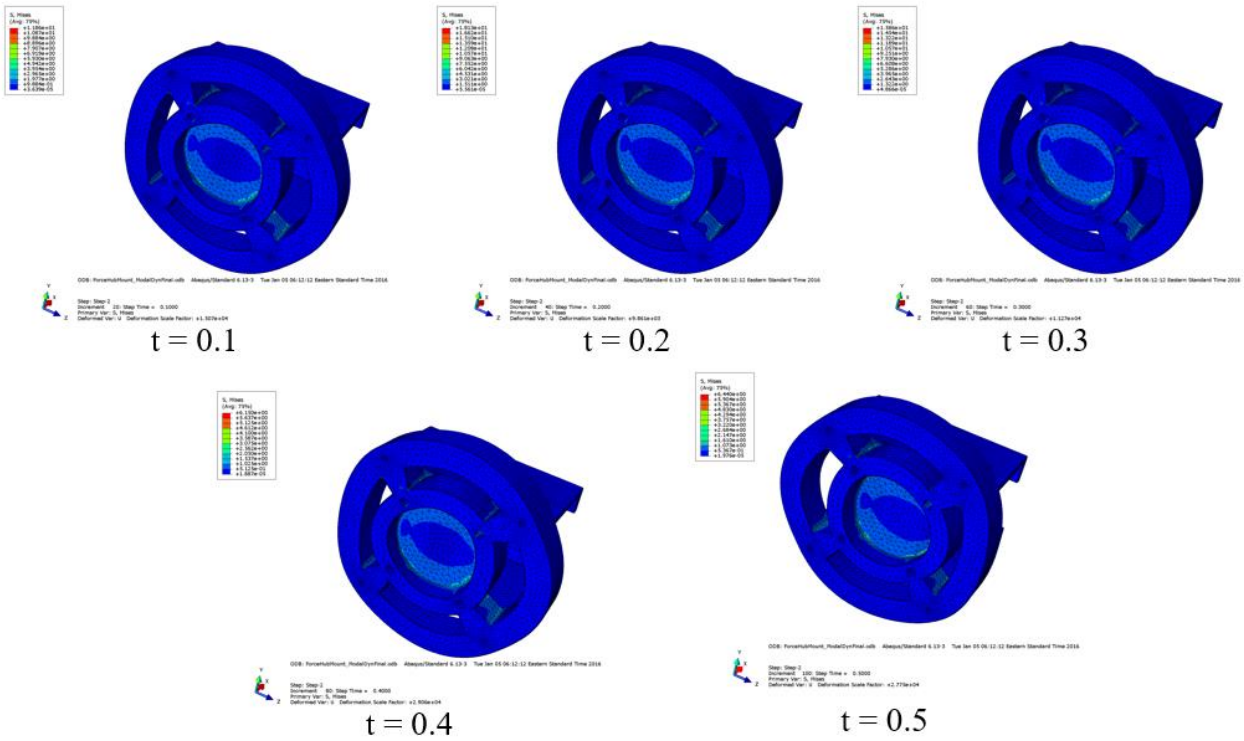

Figure 54: Modal Dynamic Analysis - Force Hub Mount - Stress Contours at t = 0.1, 0.2, 0.3, 0.4, and 0.5 (Max. Value = 18.3 MPa)

Table 11: Eigen Frequencies for Force Hub Mount

Mode	Frequency (Hz)
1	1697.7
2	2040.8
3	2520.5
4	2670.8
5	3464.4
6	3492.9
7	3576.0
8	3589.4
9	3941.2
10	3961.7

B. 2 Front Box:

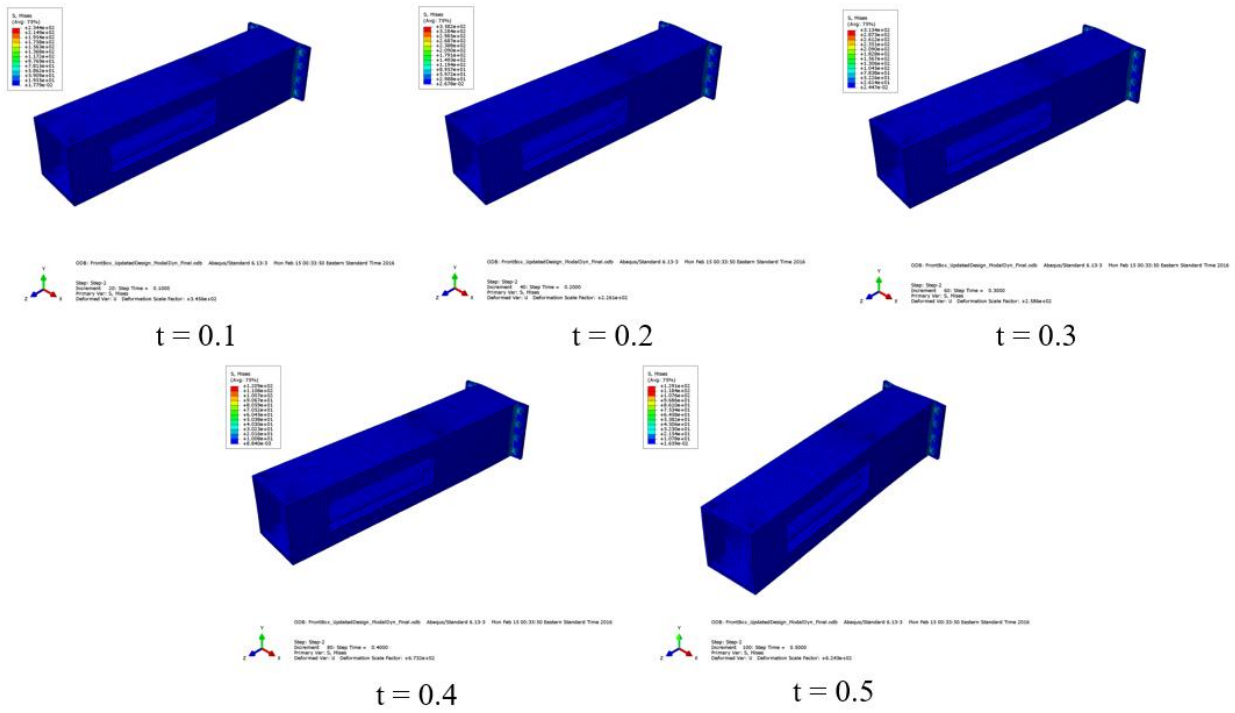

Figure 55: Modal Dynamic Analysis - Front Box - Stress Contours at t = 0.1, 0.2, 0.3, 0.4, and 0.5 (Max. Value = 359.9 MPa)

Table 12: Eigen Frequencies for Front Box

Mode	Frequency (Hz)
1	151.71
2	210.68
3	662.44
4	1136.7
5	1139.7
6	1199.9
7	1530.8
8	1848.0
9	1903.1
10	2238.5

B. 3 Beam:

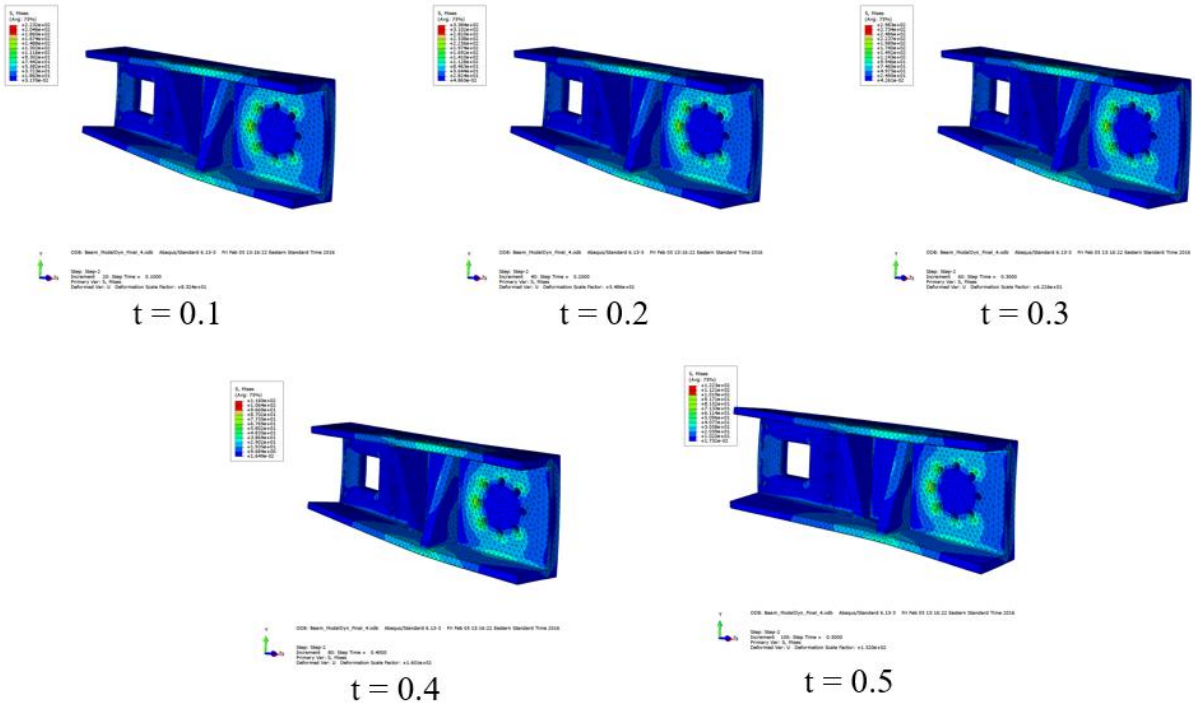

Figure 56: Modal Dynamic Analysis - Beam - Stress Contours at t = 0.1, 0.2, 0.3, 0.4, and 0.5 (Max. Value = 340.1 MPa)

Table 13: Eigen Frequencies for Beam

Mode	Frequency (Hz)
1	286.40
2	355.72
3	658.18
4	1002.6
5	1421.8
6	1488.5
7	1720.8
8	1826.9
9	1935.1
10	2030.7

B. 4 Supporting Plates:

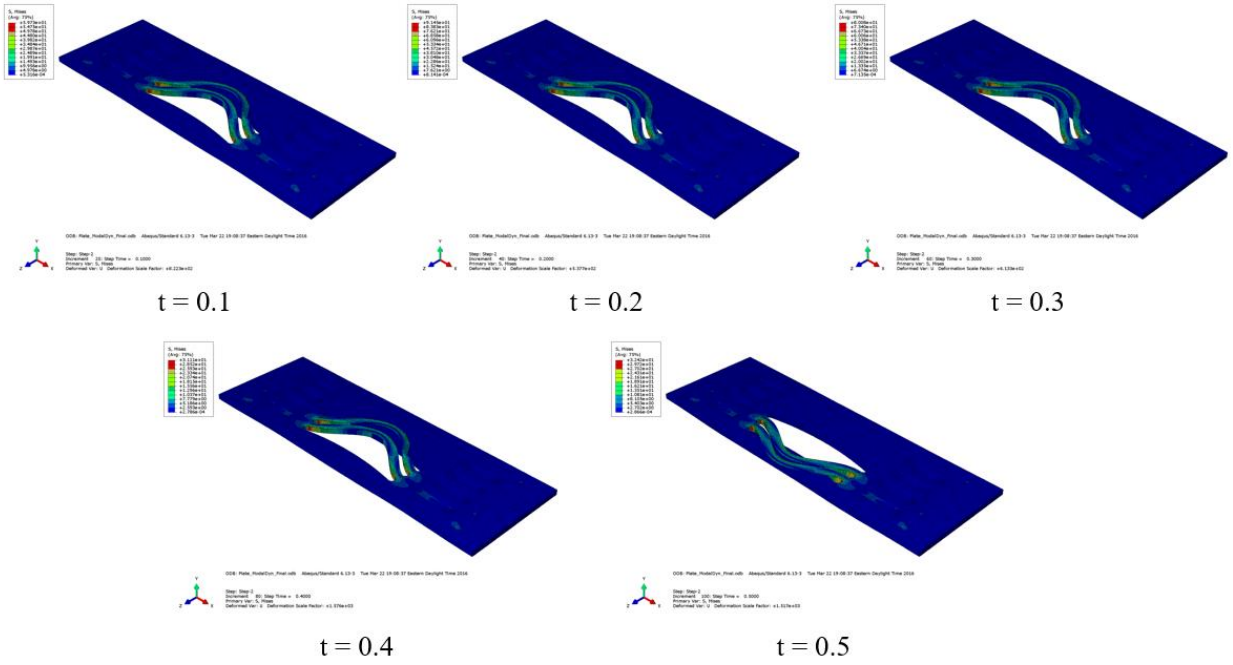

Figure 57: Modal Dynamic Analysis - Supporting Plates - Stress Contours at t = 0.1, 0.2, 0.3, 0.4, 0.5 (Max. Value = 91.45 MPa)

Table 14: Eigen Frequencies for Supporting Plates

Mode	Frequency (Hz)
1	102.49
2	162.74
3	275.39
4	337.84
5	376.04
6	425.46
7	481.62
8	533.83
9	634.90
10	757.82

B. 5 Rear Box

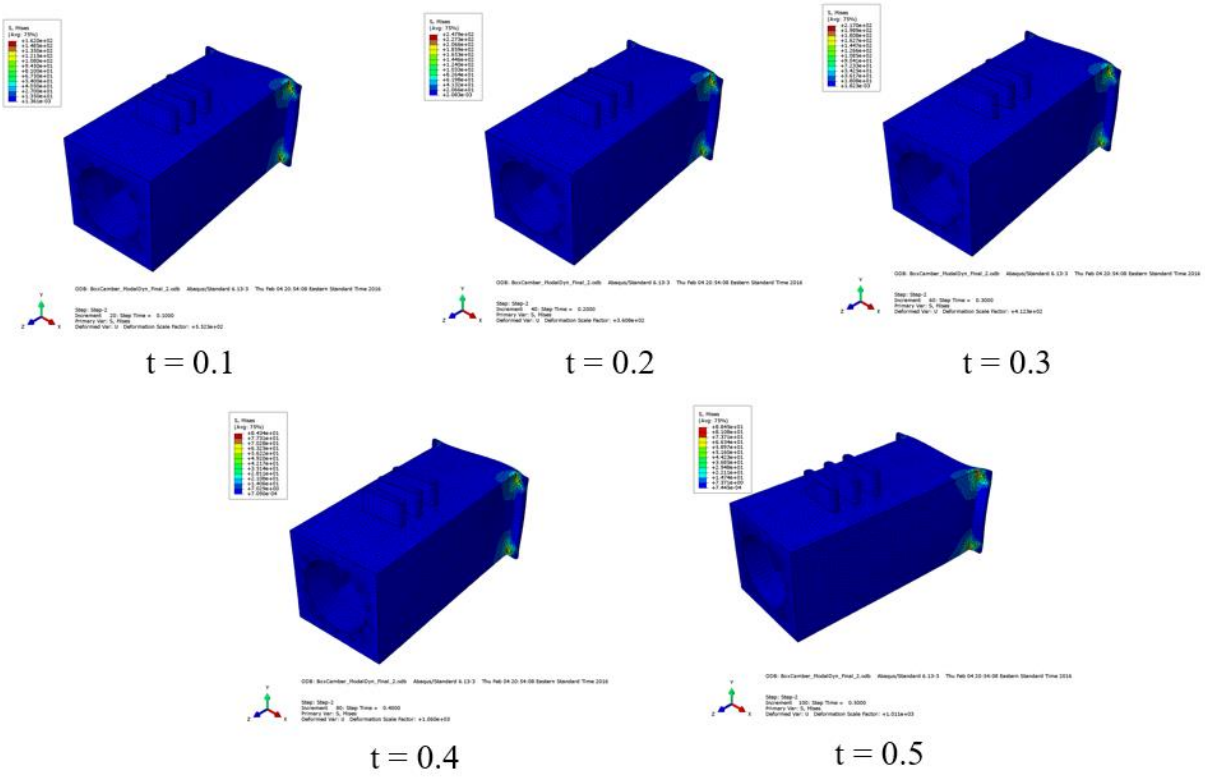

Figure 58: Modal Dynamic Analysis - Rear Box - Stress Contours at t = 0.1, 0.2, 0.3, 0.4, and 0.5 (Max. Value = 248.1 MPa)

Table 15: Eigen Frequencies for Rear Box

Mode	Frequency (Hz)
1	284.41
2	334.91
3	699.16
4	937.55
5	940.88
6	960.25
7	973.28
8	1030.8
9	1108.1
10	1275.6

B. 6 Reaction Rod Collar:

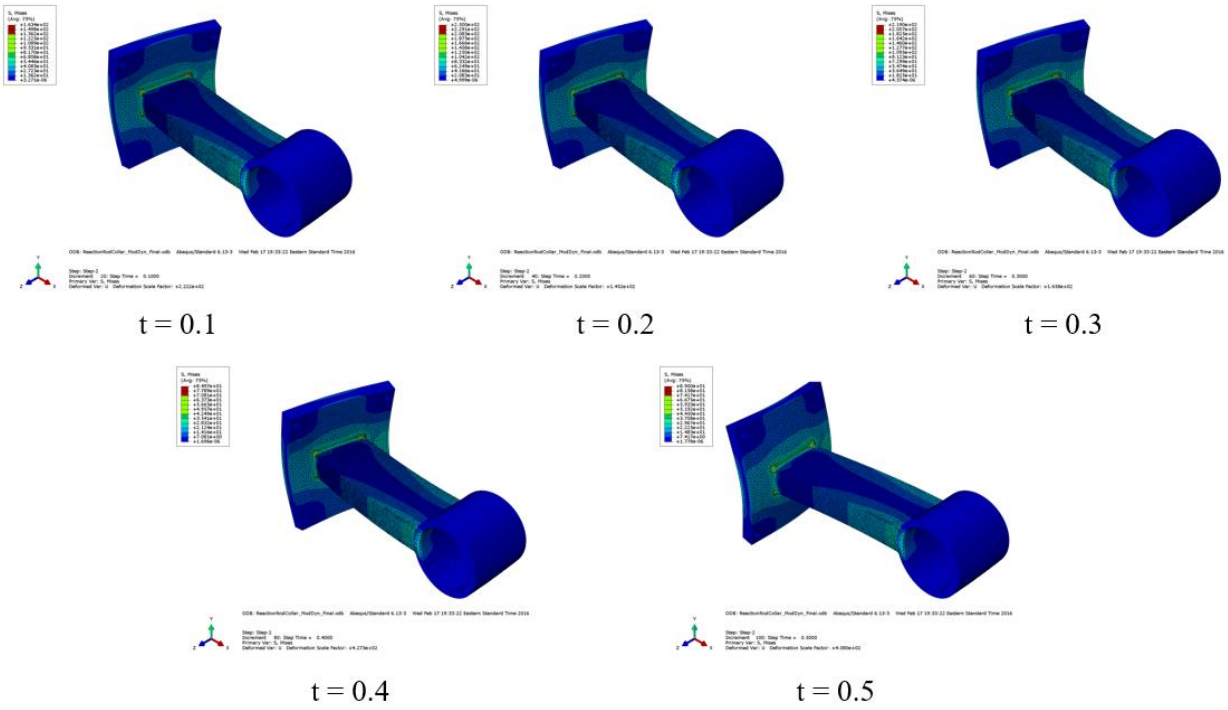

Figure 59: Modal Dynamic Analysis - Reaction Rod Collar - Stress Contours at t = 0.1, 0.2, 0.3, 0.4, 0.5 (Max. Value = 250 MPa)

Table 16: Eigen Frequencies for Reaction Rod Collar

Mode	Frequency (Hz)
1	226.78
2	495.00
3	552.46
4	1082.9
5	1831.0
6	2024.0
7	2803.0
8	3535.0
9	3939.5
10	4532.2

APPENDIX C: Additional Modal Results

The supporting brackets and plate used to mount the tire positioning mechanism were analyzed separately from the modal perspective. The plate in this assembly is bolted on linear bearings which are mounted on the machine base. Instead of analyzing the entire tire positioning mechanism with the parts in the tire positioning assembly, a plate with equivalent mass was modeled and used for the analysis. The equivalent plate was assumed to be made of steel (with density = 7900 kg/m^3). The volume of the plate was calculated based on the material and the mass of the tire positioning mechanism. The linear bearings were modeled as spring elements to take into account the deformation in the lateral direction. The modal analysis was carried out using the similar approach mentioned in the finite element analysis section. The results of the analysis are shown below:

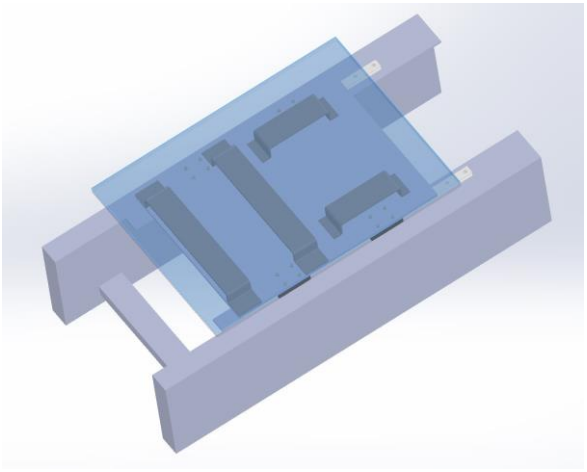

Figure 60: Equivalent Plate Arrangement

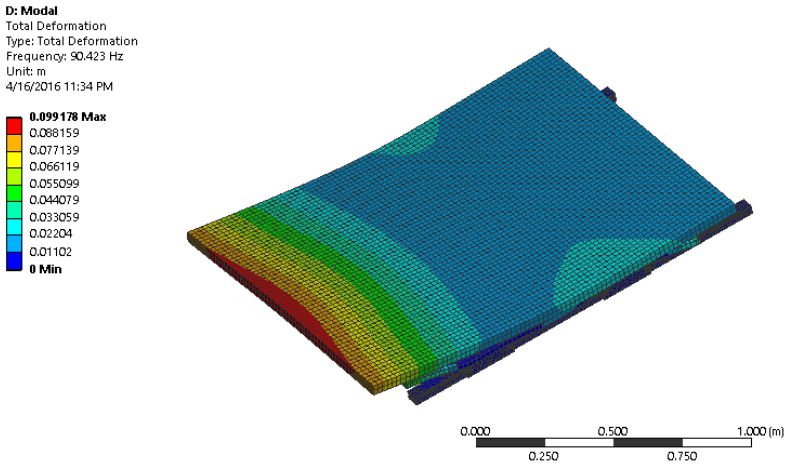

Figure 61: 1st Mode Shape for Equivalent Plate Analysis (Eigen Frequency = 90.4 Hz)

Table 17: Eigen Frequencies for Equivalent Plate Modal Analysis

Mode	Frequency (Hz)
1	90.423
2	125.39
3	138.72
4	152.14
5	170.56
6	194.01
7	206.27
8	234.82
9	257.73
10	266.39

APPENDIX D: Tire Wheel Assembly

Some additional components had to be designed to accommodate the wheel force transducer from Michigan Scientific. The sequence in which the tire is mounted on the tire positioning mechanism is shown below:

The wheel hub was mounted on the front face of the force hub mount using the 4 bolt holes seen in the figure below. This member allows the tire to rotate freely on the tire positioning mechanism.

Figure 62: Wheel Hub -Taken from Auto Parts Warehouse: Centric CE402.67019E

An adapter designed to bolt the wheel to the wheel hub was designed to accommodate a 5X4.5" lug pattern of wheel rims. The adapter was designed using aluminum and is shown in the figure below:

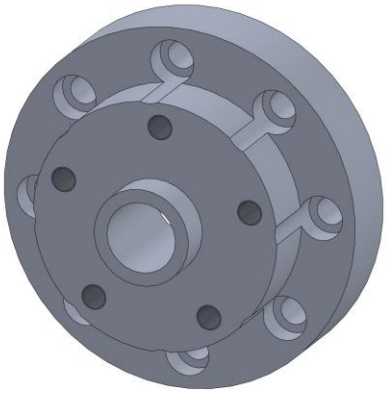

Figure 63: Aluminum Adapter

The hub adapter from the wheel force transducer assembly is bolted using the 5 lug bolt pattern on the aluminum adapter. The assembly and the individual components for the wheel force transducer have been shown in the figure below:

Figure 64: Wheel Force Transducer Assembly – Taken from Michigan Scientific – WFT Presentation

APPENDIX E: Manufactured Parts and Assemblies

The machine is in the process of being assembled and below are a few pictures of the individual parts of the mechanism being manufactured.

E.1 Reaction Rod Assembly

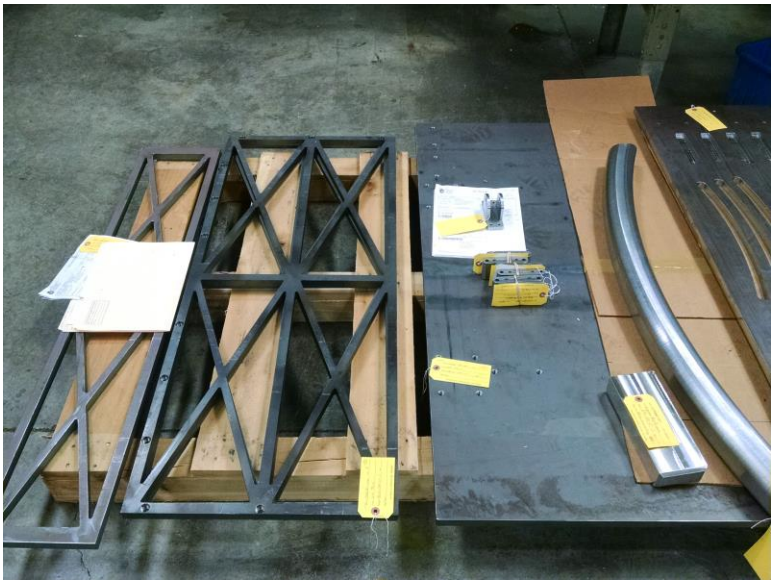

Figure 65: Bottom and Back Panels, Rod - Reaction Rod Assembly

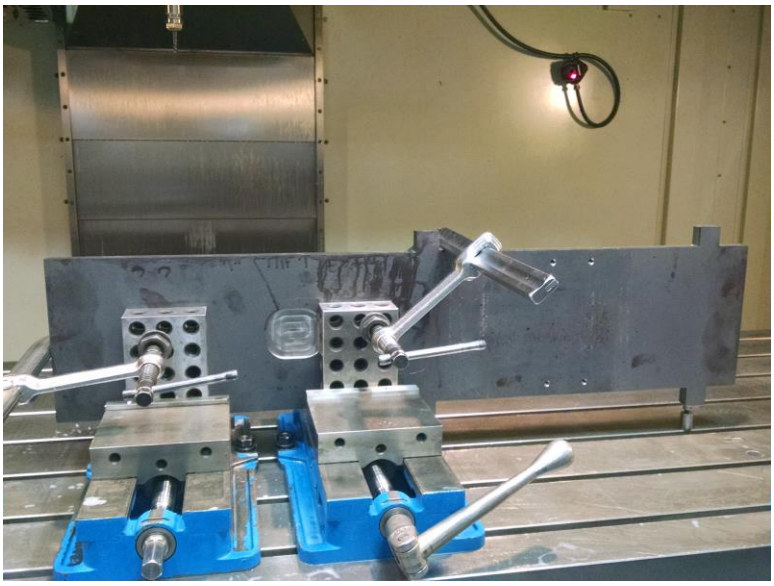

Figure 66: Vertical Panel - Reaction Rod Assembly

Figure 67: Vertical Panel (Actuator Side) - Reaction Rod Assembly

E.2 Force Hub Mount

The front flange for the force hub mount is shown in the figure below. The central boss and the flanges (which go around the box) will be assembled using dowels and bolts.

Figure 68: Force Hub Mount Front Flange

E.3 Tire Positioning Mechanism Supporting Assembly

The supporting brackets and plate shown below will be mounted on the linear bearings on the machine base to accommodate different tire sizes on the machine and for applying normal load on the tires.

Figure 69: Supporting Structure for the Tire Positioning Mechanism

APPENDIX F: Tire Terminologies and Conventions

The orientation of the tire on the machine and all the forces and moments acting on it have been considered in accordance to the SAE standard conventions. The SAE standards for tire testing ask for the force and moment sign conventions and tire terminologies to be consistent with the SAE Vehicle Dynamics Terminology J670.

The SAE tire axis system has been shown below:

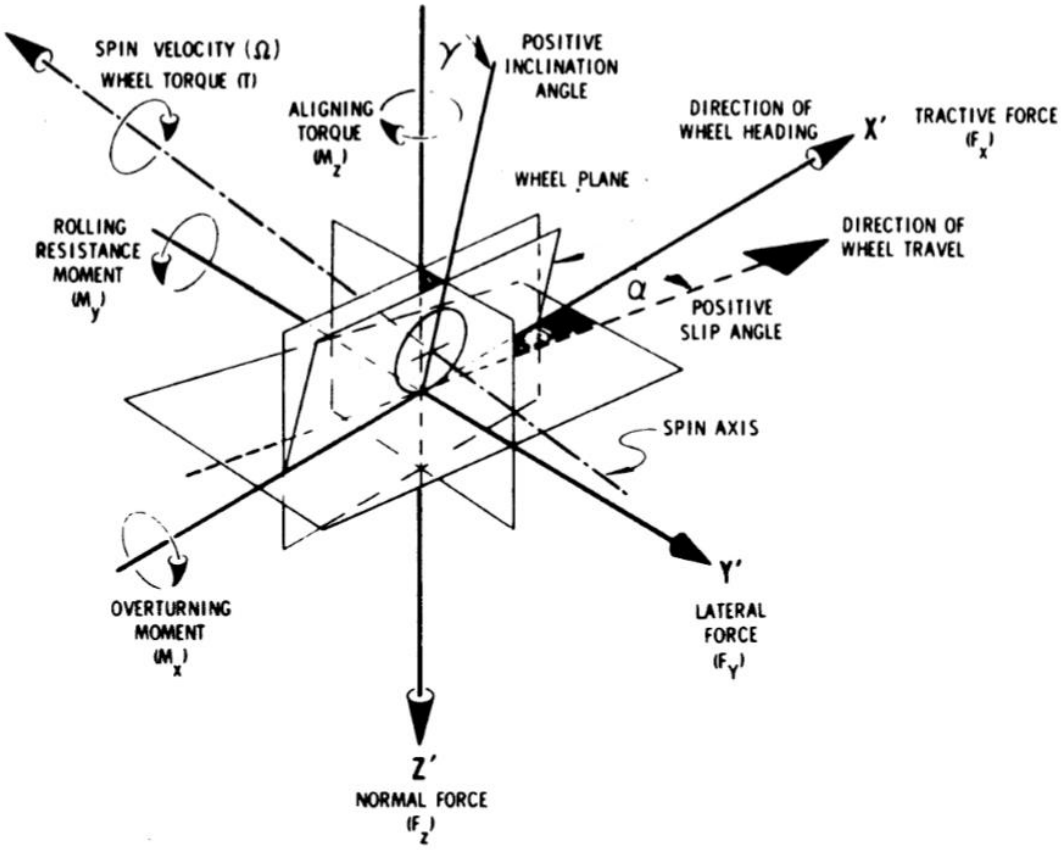

Figure 70: SAE Tire Axis System

(SAE Standard J1107: Laboratory Testing Machines and Procedures for Measuring the Steady State Force and Moment Properties of Passenger Car Tires)

According to the SAE convention, the origin of the coordinate system is placed at the center of the tire contact patch. The X axis is the intersection of the wheel plane and the road plane with positive in the direction of wheel travel. The Z axis is oriented vertical, normal to the X axis, with positive being directed downwards. The Y-axis is oriented normal to X and Z axis, and is normal to the wheel plane. It is oriented such that the system is orthogonal and right-handed.

Tire Terminologies:

Slip angle (α): It is the angle made by the X-axis with the direction of travel of the tire.

Camber or Inclination angle (γ): It is the angle measured between the Z-axis and wheel plane.

Loaded Radius (R_L): It is the value of radius measured in the wheel plane from the wheel center to the tire contact patch.

Effective Rolling Radius (R_E): It is the ratio of the wheel linear velocity (in the longitudinal direction) to the wheel spin velocity.

Tire Forces:

Longitudinal Force (F_X): It is the total force on the tire in the direction of X-axis.

Rolling Resistance Force: It is the force equivalent to the energy lost by the tire in overcoming friction and hysteresis losses.

Lateral Force (F_Y): It is the total force acting on the tire in the direction of Y-axis.

Slip Angle Force: This force is the value of lateral force obtained at zero camber angle after the forces due to plysteer and conicity have been subtracted.

Camber Force: This force is the value of lateral force obtained at zero slip angle after the forces due to plysteer and conicity have been subtracted.

Normal Force (F_Z): It is the force acting on the tire in the direction of Z-axis.

Tire Moments:

Overturning Moment (M_X): It is the moment acting on the tire which tends to rotate the tire about X axis.

Rolling Resistance Moment (M_Y): It is the moment which acts on the tire about Y-axis.

Aligning Moment (M_Z): The tire moment acting on the tire about the Z-axis.

Wheel Torque: The external torque applied on the wheel to rotate it about the spin axis.